THE TECTONIC STYLE OF THE KEWEENAWAN DEFORMATION

By

Robert Thomas Cunniff

A THESIS

Submitted to
Michigan State University
in partial fulfillment of the requirements
for the degree of

MASTER OF SCIENCE

Department of Geological Sciences

1988

ABSTRACT

THE TECTONIC STYLE OF THE KEWEENAWAN DEFORMATION

By

Robert Thomas Cunniff

The orientations of the rocks within the Lake Superior Basin define the Lake Superior Syncline (Chase and Gilmer, 1973). Deformation models which account for the rifting event must also take into consideration the compressional features exhibited by this syncline and structures surrounding it. Various models have advantages and disadvantages.

This work attempts to constrain the stresses on the midcontinental crust. Measurements made in some of the deeper interflow Keweenawan rocks indicate a small amount of compression in an essentially north-south orientation, as recorded by change of shape in pebbles and sand grains. This is supported by the orientations of mineralized fractures which are consistent with extensional fractures due to loading.

A closure/compression direction in this orientation tends to refute an impactogen or sheared origin for the original rift system. A tectonic model with separating plates around a pole of rotation or failed triple junction origin is suggested.

This work is dedicated to my parents,

Leo and Ellen

ACKNOWLEDGMENTS

I would like to acknowledge and thank my advisor, Bill Cambray, for his guidance and support during my graduate school experience. I have learned much from him in the classroom, laboratory, and in the field, not the least of which is to always lock your hotel room door when retiring from fieldwork.

I would also like to thank my committee members, Duncan Sibley, Michael Velbel and John Wilband, for their interest and advice on my thesis topic, as well as their teachings in the classroom. I am also indebted to all my other professors for sharing their knowledge with me, and Loretta, Cathy, and Mona from the geology office for their assistance.

My fellow students in the department, both graduate and undergraduate, also deserve my thanks. Paul Carter, Dave Westjohn, and Bill Sack are thanked for their discussions on our mutual structural interests, both liquid and solid. Tim Flood, John Nelson, Jim Mills, Dave Cook, and Mike Miller are all thanked for their friendship, especially during my formative, early years. Frank Rabbio, Steve Young, John Gobins, Greg Foote and many others are also thanked for their companionship.

I must also thank all the innumerable geologists I have come to know during my education. Most notable among them is Art Goldstein, who guided me during my undergraduate days, and who likes shaving cream on maroon vans. Jim Reynolds is also thanked, for having a nice sofa.

Finally I would like to thank my parents, Leo and Ellen, for making my education possible. I will always appreciate their unending encouragement and support.

TABLE OF CONTENTS

LIST OF TABLES

LIST OF FIGURES

INTRODUCTION 1

GEOPHYSICAL DATA 2

KEWEENAWAN STRATIGRAPHY 5

Sibley Group 9

Bessemer, Nopeming, and Puckwunge Formations 9

South Range and Portage Lake Volcanics 10

Oronto Group 11

Jacobsville and Bayfield Sandstones 12

PRE-KEWEENAWAN GEOLOGY AND ITS EFFECTS ON RIFTING 12

STRUCTRE 13

TECTONIC MODELS 16

METHODS 22

RESULTS 25

CONCLUSIONS 54

APPENDIX A: Strain measurements from samples 55

REFERENCES 58

LIST OF TABLES

TABLE 1. Finite strain axis values for samples 39

TABLE 2. Mean fracture orientation on each of the three planes per sample 49

TABLE 3. Outcrop fractures along north shore of the Keweenawan Peninsula. 50

TABLE 4: Measured (Input) and calculated (Output) strain axis orientations. 56

LIST OF FIGURES

Figure 1. (from Hinze and others, 1982). Simple Bouger gravity anomaly map of Lake Superior. 3

Figure 2. (from Hinze and others, 1982). Total magnetic-intensity anomaly map of Lake Superior. 4

Figure 3. (from Hinze and others, 1982). Observed Bouger gravity and total magnetic-intensity anomaly profiles across western Lake Superior. Related crustal cross section shows assumed densities in g/cm^3. 6

Figure 4. (from Hinze and others, 1982). Observed Bouger gravity and total magnetic-intensity anomaly profiles across eastern Lake Superior. Related crustal cross section shows assumed densities in g/cm^3. 6

Figure 5. (from Behrendt and others, 1988). GLIPMSE deep seismic profile across eastern Lake Superior. 7

Figure 6. (from Daniels, 1982). Generalize geologic column of Keweenawan rocks in the Lake Superior region. 8

Figure 7. (from Klasner and others, 1982). Generalized tectonic map showing major tectonic units in the area surrounding the Midcontinent Rift System. Location of rift shown by shaded area that outlines associated gravity anomaly. 14

Figure 8. (from Green, 1982). Geological map of Lake Superior area. Short dashed lines - present limit of Keweenaw lavas. Heavy dashed lines - faults. Unpatterned and areas - pre-Keweenawan rocks. Cross-hatched and checked - lavas. Dots - major intrusive bodies. Horizontal lines - Upper Keweenawan sediments overlying lavas. 15

Figure 9. (from Green, 1982). Generalized interpretive geological cross section through figure 8 along AB, with associated Bouger gravity anomaly. LMPC-Lower and Middle Precambrian rocks: OS-Osler Group; PM-Powder Mill Group; NSR-North Shore reversed polarity lavas; NSN-North Shore normal polarity lavas; PLV-Portage Lake Volcanic; DG-Duluth Complex; UKS-Upper Keweenawan sedimentary rocks. 15

Figure 10. (from Green, 1982). Generalized interpretive geological cross section through figure 8 along CD, with associated Bouger gravity anomaly. Key same as Figure 9. 15

LIST OF FIGURES (continued)

Figure 11. (from , 1982). Geological map of Lake Superior region showing possibilities for a failed third arm of a triple junction rift geometry. 17

Figure 12. (from White, 1965). Interpreted tectonic models for crustal structure in the Midcontinent Rift. 19

Figure 13. Interpreted tectonic model for crustal structure in the Midcontinent Rift. 19

Figure 14. Study area showing sample groupings. 23

Figure 15. Stereo net plot of sample MR1. Left hand plot is of strain axes as they are in outcrop. Right hand plot has had structural dip removed by rotating -54° around 295, 00. 26

Figure 16. Stereo net plot of sample MR2. Left hand plot is of strain axes as they are in outcrop. Right hand plot has had structural dip removed by rotating -41° around 290°, 00°. 27

Figure 17. Stereo net plot of sample MR2SL. Left hand plot is of strain axes as they are in outcrop. Right hand plot has had structural dip removed by rotating -41° around 290°, 00°. 28

Figure 18. Stereo net plot of sample MR3. Left hand plot is of strain axes as they are in outcrop. Right hand plot has had structural dip removed by rotating -49° around 290°, 00°. 29

Figure 19. Stereo net plot of sample MR9. Left hand plot is of strain axes as they are in outcrop. Right hand plot has had structural dip removed by rotating -46° around 285°, 00°. 30

Figure 20. Stereo net plot of sample MR10. Left hand plot is of strain axes as they are in outcrop. Right hand plot has had structural dip removed by rotating -40° around 280°, 00°. 31

Figure 21. Stereo net plot of sample MR10SL. Left hand plot is of strain axes as they are in outcrop. Right hand plot has had structural dip removed by rotating -40° around 280°, 00° 32

Figure 22. Stereo net plot of sample PU1. Left hand plot is of strain axes as they are in outcrop. Right hand plot has had structural dip removed by rotating -99° around 301°, 00°. 33

Figure 23. Stereo net plot of sample BH1. Left hand plot is of strain axes as they are in outcrop. Right hand plot has had structural dip removed by rotating 51° around 065°, 00°. 34

LIST OF FIGURES (continued)

Figure 24. Stereo net plot of sample BH1SL. Left hand plot is of strain axes as they are in outcrop. Right hand plot has had structural dip removed by rotating 51° around 065°, 00°. 35

Figure 25. Stereo net plot of sample PL1. Left hand plot is of strain axes as they are in outcrop. Right hand plot has had structural dip removed by rotating 71° around 071°, 00°. 36

Figure 26. Contoured calculated strain axes (1% area radius) stereo net plot of all "MR" and "PU" samples. Left hand plot is of strain axes as they are in outcrop. Right hand plot has had structural dip removed by rotating -49° (mean dip) around 287°, 00° (mean strike). 37

Figure 27. Stereo net plot of samples "BH" and "PL". Left hand plot is of strain axes as they are in outcrop. Right hand plot has had structural dip removed by rotating 57° (mean dip) around 066°, 00° (mean strike). 38

Figure 28. Stereo net plot of fractures from sample MR1. Squares represent fractures on MR1-1, triangles for MR1-2, and crosses for MR1-3. Solid circles are the mean orientations of the fracture traces for each plane. The plotted plane represents best fit plane of fracture. 41

Figure 29. Stereo net plot of fractures from sample MR2. Squares represent fractures on MR2-1, crosses for MR2-2, and triangles for MR2-3. Solid circles are the mean orientations of the fracture traces for each plane. The plotted plane represents best fit plane of fracture. 42

Figure 30. Stereo net plot of fractures from sample MR3. Squares represent fractures on MR3-1, triangles for MR3-2, and crosses for MR3-3. Solid circles are the mean orientations of the fracture traces for each plane. The plotted plane represents best fit plane of fracture. 43

Figure 31. Stereo net plot of fractures from sample MR9. Squares represent fractures on MR9-1, triangles for MR9-2, and crosses for MR9-3. Solid circles are the mean orientations of the fracture traces for each plane. The plotted plane represents best fit plane of fracture. 44

Figure 32. Stereo net plot of fractures from sample MR10. Squares represent fractures on MR10-1, triangles for MR10-2, and crosses for MR10-3. Solid circles are the mean orientations of the fracture traces for each plane. The plotted plane represents best fit plane of fracture. 45

LIST OF FIGURES (continued)

Figure 33. Stereo net plot of fractures from sample PU1. Squares represent fractures on PU1-1, triangles for PU1-2, and crosses for PU1-3. Solid circles are the mean orientations of the fracture traces for each plane. The plotted plane represents best fit plane of fracture. 46

Figure 34. Stereo net plot of fractures from sample BH1. Squares represent fractures on BH1-1, triangles for BH1-2, and crosses for BH1-3. Solid circles are the mean orientations of the fracture traces for each plane. The plotted plane represents best fit plane of fracture. 47

Figure 35. Stereo net plot of fractures from sample PL1. Squares represent fractures on PL1-1, triangles for PL1-2, and crosses for PL1-3. Solid circles are the mean orientations of the fracture traces for each plane. The plotted plane represents best fit plane of fracture. 48

Figure 36. Contoured stereo net plot of fractures found along the Keweenaw Peninsula north shore, near mouth of Eagle River. 51

Figure 37. Contoured stereo net plot of fractures found along the Keweenaw Peninsula north shore, near Hebard Park. 52

Figure 38. Contoured stereo net plot of fractures found along the Keweenaw Peninsula north shore, near Copper Harbor. 53

INTRODUCTION

The structural basin which Lake Superior occupies is composed of Proterozoic sedimentary, volcanic and intrusive rocks which unconformably overlie older Proterozoic and Archean rocks. This sequence has been termed the Keweenawan (Proterozoic Y), with its type locality being the Keweenaw Peninsula of Northern Michigan The Keweenawan sequence is the exposed portion of a major North American tectonic feature known as the Midcontinent Rift System (MRS).

The rift system can be traced by a pronounced gravity and magnetic high resulting from the mafic igneous rocks which accompanied rifting. From the Lake Superior region the rift extends more than 2,000 km southwest to Kansas, and southeast into the basement rocks of the Michigan Basin, forming an arcuate anomaly with the concavity pointing southward. This midcontinent gravity high directly corresponds to the MRS. This Midcontinent Gravity and Magnetic Anomaly is the largest geophysical feature in North America.

Stratigraphically, petrologically and geophysically this feature resembles what would be expected for a failed rift system which extended the continental crust 1.1 Gyr ago. The ambiguity of structural features, including compressional faults, makes it difficult to agree on a specific model for deformation of the Proterozoic craton and Keweenawan series. Several different models can be used to explain the observed features: these range from classical rifting interpretations to very different, opposite sense of motion, compressional models.

Tectonic models, which will be discussed later, must account for both the classic extensional features as well as the compressional ones associated with this particular

rift. The two sets of features are either contemporaneous, or a separate compressional phase must have been superimposed on the extensional elements.

This study's contribution to the deformation problem of the Keweenawan attempts to define the finite strain recorded in some of the rift sediments. By comparing strain axis and fracture orientations an interpretation can be made regarding the directions of stress which could have caused the deformation.

Geophysical Data:

Traced by gravity, the MRS extends southwest beneath younger Phanerozoic units, from the Lake Superior region into central Kansas, as well as southeastward underneath the Michigan Basin and possibly northward into Canada as part of a failed triple junction (Chase and Gilmer, 1973). (See Figure 1, Simple Bouger gravity anomaly map of Lake Superior). A triple junction in continental material is generally considered to be the first stage of rift development. It is anticipated that the least-developed arm of the junction fails, resulting in a more "linear" rift, evolving eventually into a spreading ridge of oceanic crustal affinity.

The entire Lake Superior region is modeled as having an abnormally dense character (Hinze, et al, 1982) which is interpreted as a result of intrusions emplaced in a zone of extension along the basin axis. This central axis of the basin corresponds to a magnetic minimum which might be due to the greater thickness of sediment over the magnetic bodies. (See Figure 2, total magnetic-intensity map of Lake Superior). Both Figure 1 and 2 show how Midcontinent Rift associated features also crosscut pre-existing Precambrian geophysical patterns.

The result of removing the mass deficiency of the overlying clastic rocks of the Jacobsville-Bayfield Group yields a residual gravity map which shows negative anomalies surrounding a central positive one. The amplitude of the minima suggest a regional negative anomaly as a result of crustal thickening under the basin (Hinze, et

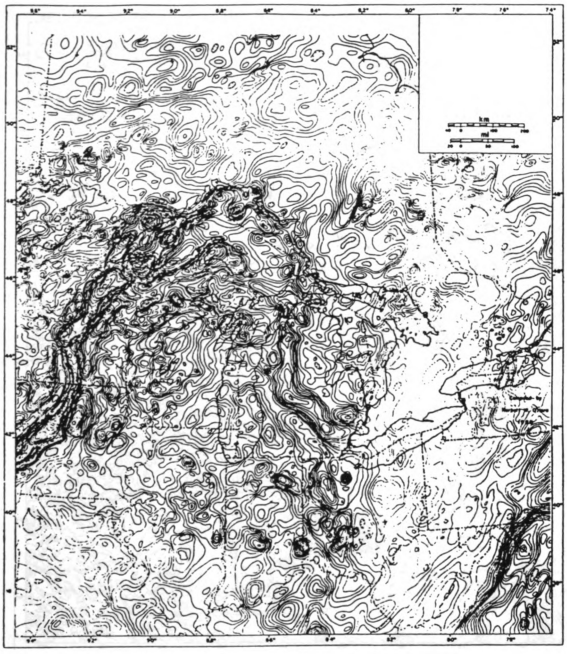

Figure 1. (from Hinze and others, 1982). Simple Bouger gravity anomaly map of Lake Superior.

Figure 2. (from Hinze and others, 1982). Total magnetic-intensity anomaly map of Lake Superior.

al, 1982). In the central and eastern portions of Lake Superior the crust may be thickened to as much as 50 km (Halls, 1982). The minima which surround the isolateepositive high for most of its length outside of the Lake Superior region are also assumed to be associated with an overall thickening of the continental crust by pluton emplacement as a result of rift mechanics.

Gravity and magnetic modeling profiles across the western and eastern portions of the lake (Figure 3 and Figure 4 respectively) show differential emplacement of high density intrusions. This would indicate rifting of the crust was more developed (vertically) in the western half, between Isle Royale and the Keweenaw Peninsula. The presence of high velocity mafic intrusions under the center of the basin is supported by many workers who use refraction data (Hinze et al. 1982, and Halls, 1982).

The most recent seismic reflection study in the Lake Superior region yields an interpretation somewhat different than older geophysical models. Behrendt, et al, 1988 with the GLIMPCE seismic reflection survey done in Lake Superior, shows as much as 32 km of rift sediments and volcanics overlying 10-15 km of continental crust thinned by 25-30 km from its original thickness of 35-40 km. At its thickest, in western Lake Superior, there appear to be 12-14 km of post volcanic clastics over up to 20 km of lavas and interbedded sediments. Figure 5 shows an interpretation of the seismic data which represents a gently folded basin sequence bounded by reverse faults. Basinward thickening of the lavas it not particularly evident.

Keweenawan Stratigraphy:

Different authors have developed their own classification systems for the rocks of the Midcontinent Rift System. This paper will use the stratigraphy as put forward by Daniels (1982), (see Figure 6), as he applies stratigraphic names from Michigan and Wisconsin to other Keweenawan rocks elsewhere in the Lake Superior region.

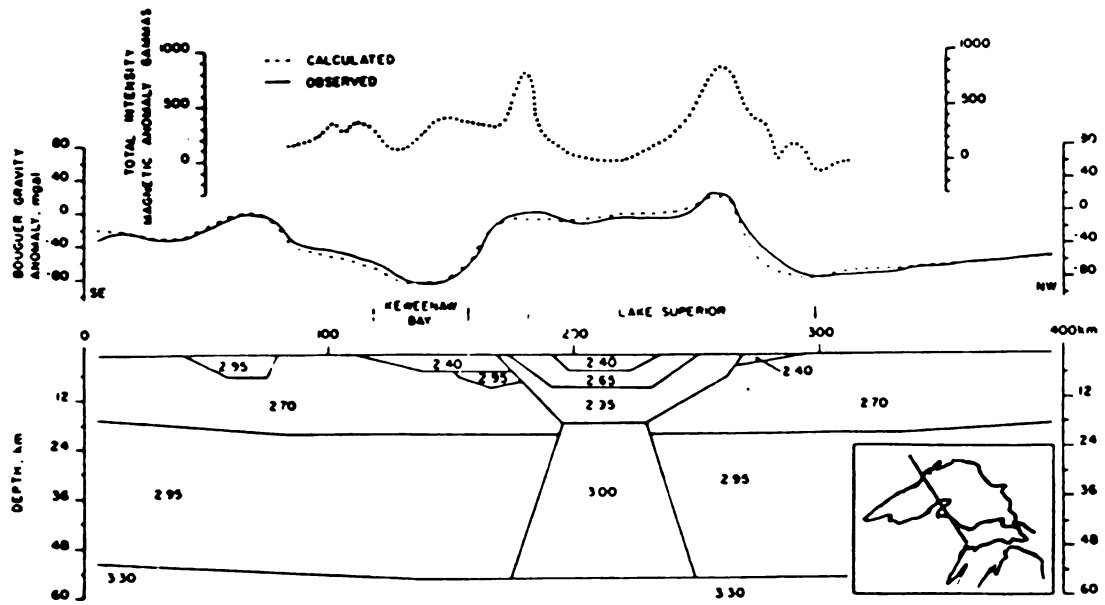

Figure 3. (from Hinze and others, 1982). Observed Bouger gravity and total magnetic-intensity anomaly profiles across western Lake Superior. Related crustal cross section shows assumed densities in g/cm^3.

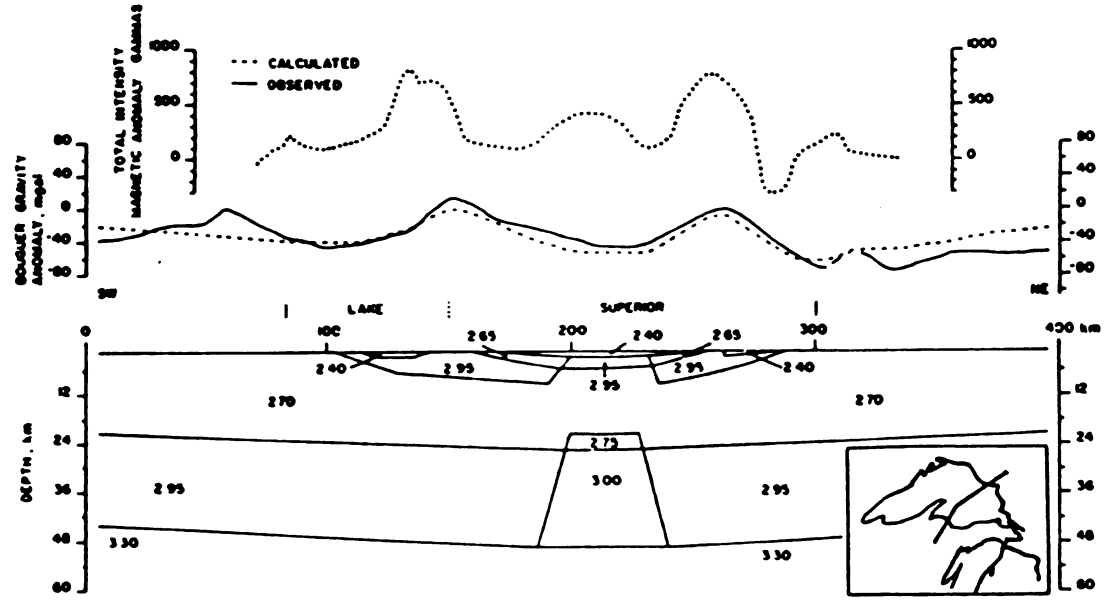

Figure 4. (from Hinze and others, 1982). Observed Bouger gravity and total magnetic-intensity anomaly profiles across eastern Lake Superior. Related crustal cross section shows assumed densities in g/cm^3.

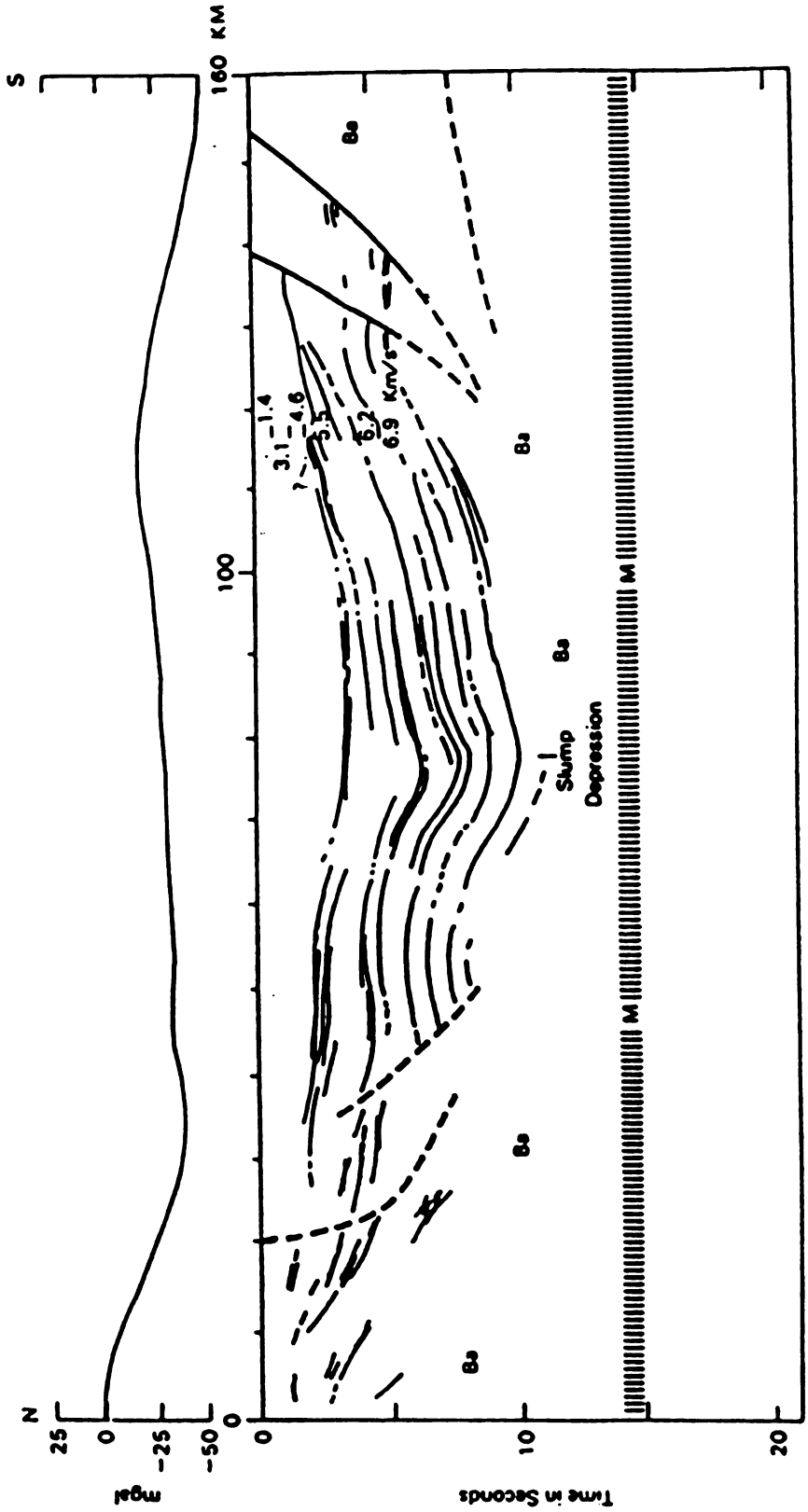

Figure 5. (from Behrendt and others, 1988). GLIPMSE deep seismic profile across eastern Lake Superior.

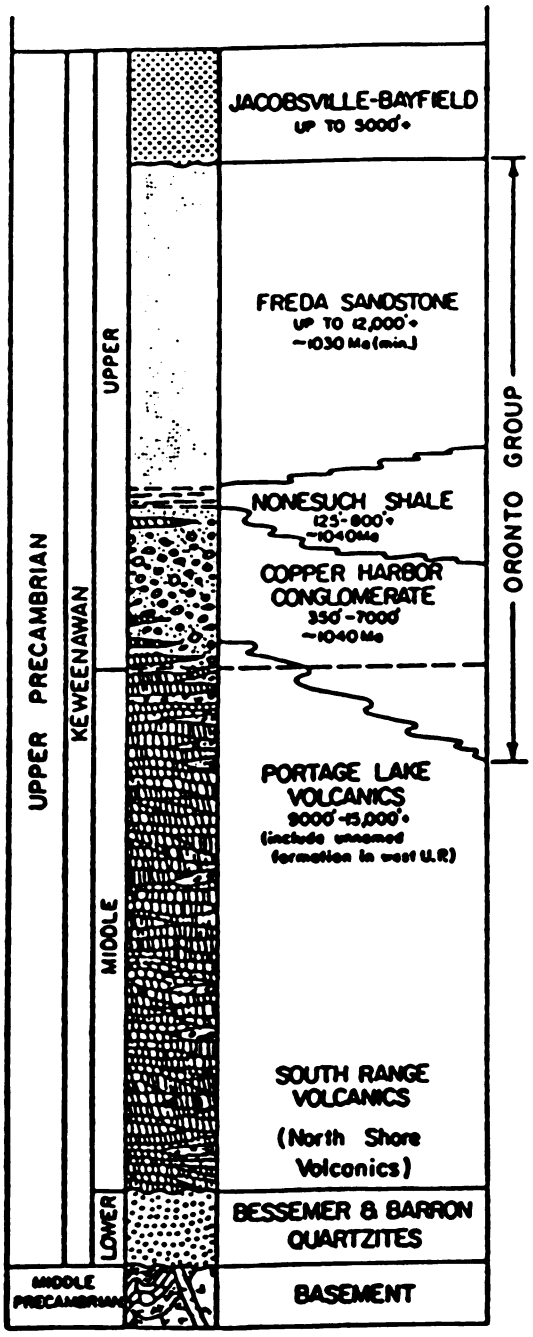

Figure 6. (from Daniels, 1982). Generalized geologic column of Keweenawan rocks in the Lake Superior region.

The oldest Keweenawan unit overlies middle Precambrian and Archean basement (discussed later) and predates volcanics in the region. Making up the Lower Keweenawan are the Sibley Group, the Neopeming Formation and the Puckwunge Formation to the western/northern side of the rift, and the Bessemer Quartzite in Michigan and Wisconsin (southern/eastern side of the rift) The Baraboo, Waterloo Sioux, Flambeau and Barron Quartzites may be related to each other, but due to minimum age requirements from cross-cutting rhyolite dike ages, and folding with low-grade metamorphism, they appear to be older than the Sibley Group and are apparently unrelated to the MRS.

Sibley Group:

The Sibley Group appears to be oldest pre-volcanic sandstone at 1.35 Ga. It appears as a braided alluvial fan on the north shore of Lake Superior. Ojakangas and Morey's (1982a), model for early Keweenawan deposition shows two basins. The older basin, containing the Sibley Group has a north-south trend and extends northward from the north shore of Lake Superior Cross-bedding paleocurrent indicators show main sediment transport directions to the south-southwest and south-southeast.

Bessemer, Nopeming, and Puckwunge Formations:

A slightly younger basin (1.2-1.1 Ga), in Ojakangas and Morey's (1982a) model, trended east-west, was located in the approximate position of Lake Superior today, and received the sediments of the Bessemer Quartzite, the Nopeming and Puckwunge formations and unamed sands of the Lower Osler Group. Soft sediment deformation at the top contact of the Bessemer and Nopeming with the overlying lava flows, as well as clastic dikes in the flows, date these sediments approximately equal in age to that of the flows (1.2-1.1 Ga).

These sands are taken to approximate lithostratigraphic equivalents. The Bessemer's bimodal-bipolar paleocurrent plots indicate either a tidally influenced

shallow marine setting, or a lacustrine environment where opposing longshore currents operate on an approximate east-west direction. The Puckwunge and Nopeming formations are unimodal and suggest fluvial environments; streams flowing southward into the basin where the Bessemer had been, or was being deposited (Ojakangas and Morey, 1982a).

South Range and Portage Lake Volcanics:

With the onset of volcanism, topography seems to have become less subdued and more complex including the development of at least seven individual basins of deposition along the rift as shown by ponded lavas (Green, 1982 and White, 1966). These lavas mark the beginning of Middle Keweenawan time and make up a pile as thick as 30,000 feet (White, 1966) and up to 400,000 km^3 in volume (Green, 1982). This pile consists of the South Range volcanics (the lower lavas) and the Portage Lake volcanics (the upper lavas).

Not shown on Figure 6 are Middle Keweenawan interflow conglomerates (generally not named as separate formations due to limited areal extent). These conglomerates sometimes make up to 24 percent of the local sections of exposure at different localities (Merk and Jirsa, 1982). They are taken to represent a hiatus in volcanism within a particular basin. These conglomerates are coarse and immature and are the detritus from three major sources: subjacent lava flows, Keweenawan flows and intrusions located at some distance from the deposition site, and pre-Keweenawan basement source rocks. This last source appears only in the youngest interflows and the formations overlying and suggests that nearby the Keweenawan sequence had been eroded through to basement, perhaps at the basin margins where cover was thinner (Merk and Jersa, 1982).

Oronto Group:

Deposition of this group's first unit, the Copper Harbor Conglomerate, marks the onset of Upper Keweenawan time. This unit is a fining upward sequence thickening basinward, and consisting predominantly of volcanic rhyolitic and mafic clasts set in a lithic greywacke matrix (Daniels, 1982). Near the basin axis the sediment may have accumulated up to 2,130 m in thickness (White, 1966). Localized lenzes of Copper Harbor Sandstone occur which appear very similar to the Conglomerate matrix (Daniels, 1982) and both are similar in composition to the interflow conglomerates, which suggests similar sources.

High energy flow-regime sedimentary structures, desication cracks and interference ripples indicate a fluctuating energy level and water depth. An alluvial fan/clastic wedge and other subenvironments are postulated as the depositional facies for this unit (Daniels, 1982). The coarse conglomerates represent braided stream, and the laminated sandstones, very small lacustrine environments. Near Copper Harbor Michigan there is a stromatolitic facies which suggests the presence of a substantial ephemeral lake.

Conformably overlying the Copper Harbor facies is the Nonesuch Shale Formation which averages 180 m in thickness and more texturally and compositional mature than older Middle Keweenawan units (Daniels, 1982). This unit also contains organic material and diagenetic carbonate nodules, suggesting a reducing, quiet water deposition, possibly of reworked Copper Harbor sediments (White, 1972). This evidence suggests a transgressive sequence over the the underlying red beds forming a lacustrine depositional system (Daniels, 1982).

The Nonesuch has a gradational upper contact with the overlying Freda Sandstone. This unit is fine grained and micaceous with variable textural and compositional maturity. In many localities the Freda exhibits a sandstone-mudstone,

cyclic sedimentation which suggests an alluvial channel fill sequence with contributions from lacustrine and possibly even marine environments (Daniels, 1982)

Jacobsville and Bayfield Sandstones:

Overlying the Oronto group are the Jacobsville and Bayfield Sandstones Paleosols along the contact indicates an erosional unconformity at the base of the 3 000 m thick Jacobsville (Kaliokoski 1982) The Bayfield Group, which is taken to be the equivilalent of the Jacobsville in eastern Minnesota and northwestern Wisconsin, is 2 100 m of flat lying quartzose and arkosic sands deposited on top of the more steeply dipping Oronto Group, indicating a post deformational deposition (Morey and Ojakangas 1982) Both sands are more mature than the underlying sediments; the Jacobsville has basal pebble conglomerates but varies from ripple-marked and cross bedded subarkoses to quartz sublithic arenites through most of its thickness (Kalliokoski, 1982), the Bayfield sands are all relatively mature arenites (Morey and Ojakangas, 1982)

Overall the Oronto Group suggests a prograding alluvial fan deepening into transgressive lacustrine and prograding braided stream environments (Daniels, 1982) The Jacobsville and Bayfield suggest a quiet tectonic regime where erosion reworked existing lithologies to deposit mature standing water and fluvial sandstones (Morey and Ojakangas, 1982).

Pre-Keeweenawan Geology and its Effects on Rifting:

The rifted area consists of two different geological provinces. The northern area is predominantly volcanic and plutonic belts alternating with gneisses not older than 3.1 Ga, which have remained a tectonically rigid block from 2.6 Ga. These rocks are part of the Superior Province of the southern Canadian Shield. The southern rocks

are as old as 3.8 Ga, and have undergone orogenies at 2.6, 1.85, and 1.76 Ga, followed by intrusion of the non-orogenic Wolf River Batholith at 1.5 GA ago (Klasner, et al, 1982).

Both areas have strong structural fabrics which trend east-northeast as large foldbelts. The rift orientation is apparently unaffected by this fabric (as can be seen in Figure 7) although it does appear to have been guided by pre-Keweenawen faults and lineaments as well as arched around the Wolf River Batholith (Klasner, et al, 1982).

The geologic contact between the Superior Province and the older (Penokean) foldbelt to the south corresponds to an abrupt change in the width of the rift, as recorded by the geophysical data, and the complexity of its structure as modeled by White, (1965). The Superior Province's associated gravity high is approximately 150 km wide, compared to a narrower 90 km for the southern portion of the rift. The wider portion may also have a more complex structure; two parallel rifts surrounding sialic blocks of crust (White, 1965), whereas the southern portion appears to be simple depositional basins arranged in linear segments.

Structure:

The structure of the Lake Superior Basin and the associated Lake Superior Syncline is relatively simple. Keweenawan rocks in northern Michigan dip steeply to the north and west, whereas the same rocks in Minnesota and Isle Royale dip shallowly to the south and east (Chase and Gilmer, 1973). Such a structure obviously describes an asymmetric syncline with its axis displaced nearer to Michigan (See Figure 8) Furthermore, the edges of the Syncline are bounded by thrust faults; the Isle Royale/Douglas Fault to the northwest, and the Keweenaw Fault to the southeast. Figures 9 and 10 provide interpreted geological cross sections from A to B, and C to D, respectively, on Figure 8.

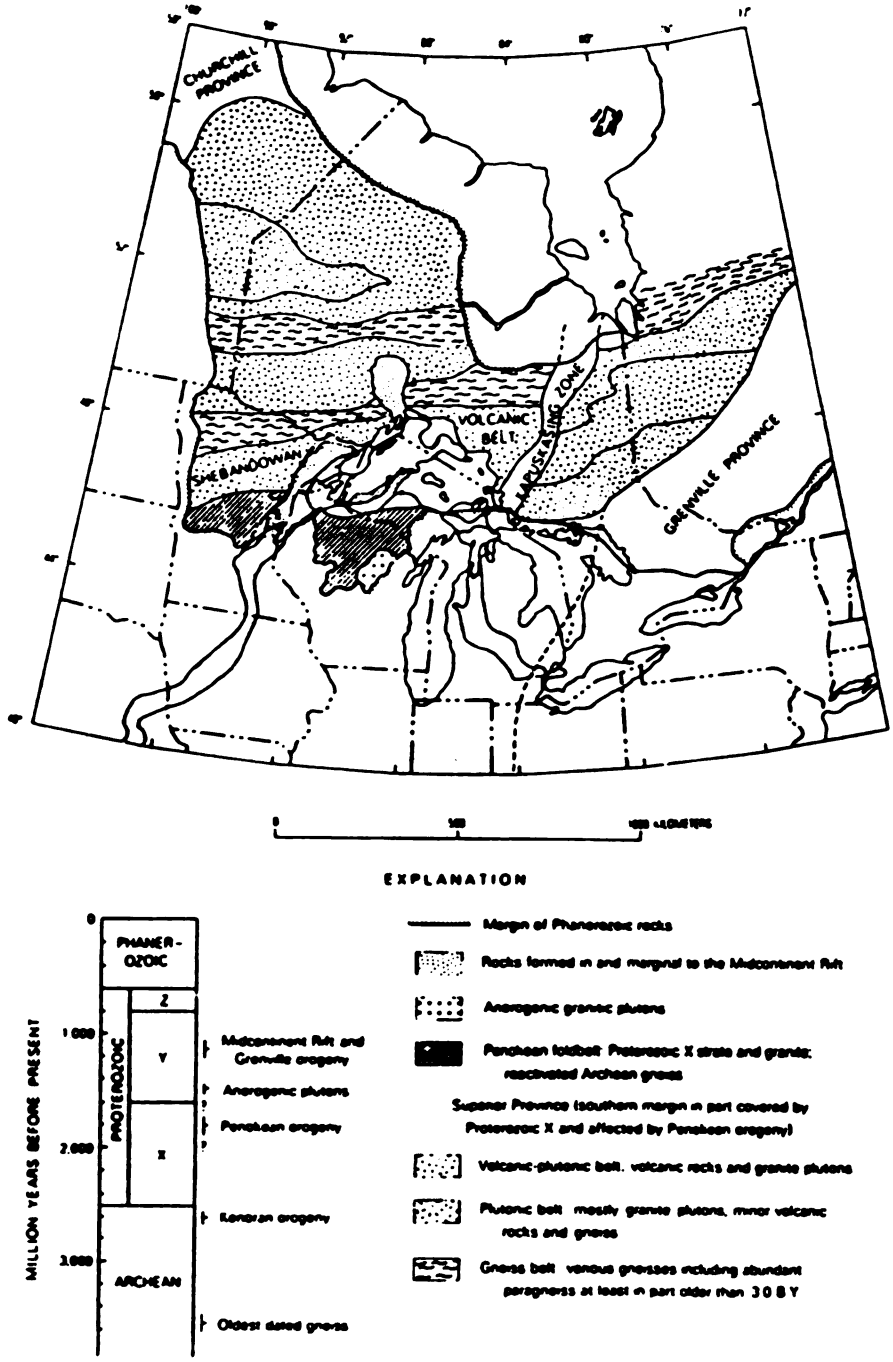

Figure 7. (from Klasner and others, 1982). Generalized tectonic map showing major tectonic units in the area surrounding the Midcontinent Rift System. Location of rift shown by shaded area that outlines associated gravity anomaly.

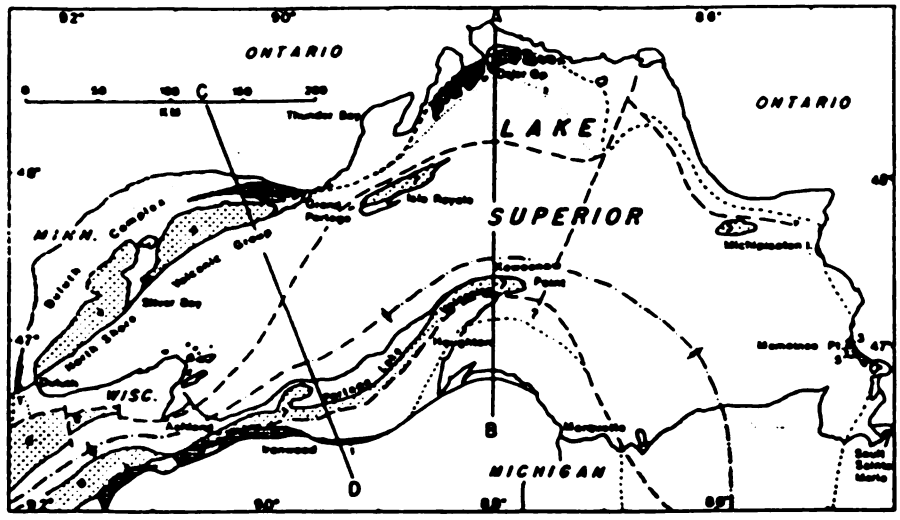

Figure 8. (from Green, 1982). Geological map of Lake Superior area. Short dashed lines - present limit of Keweenaw lavas. Heavy dashed lines - faults. Unpatterned areas - pre-Keweenawan rocks. Cross-hatched and checked - lavas. Dots - major intrusive bodies. Horizontal lines - Upper Keweenawan sediments overlying lavas.

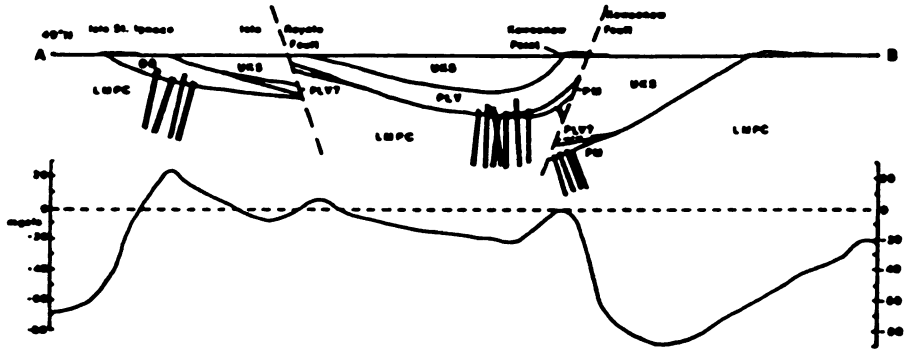

Figure 9. (from Green, 1982). Generalized interpretive geological cross section through figure 8 along AB, with associated Bouger gravity anomaly. LMPC-Lower and Middle Precambrian rocks; OS-Osler Group; PM-Powder Mill Group; NSR-North Shore reversed polarity lavas; NSN-North Shore normal polarity lavas; PLV-Portage Lake Volcanic; DG-Duluth Complex; UKS-Upper Keweenawan sedimentary rocks.

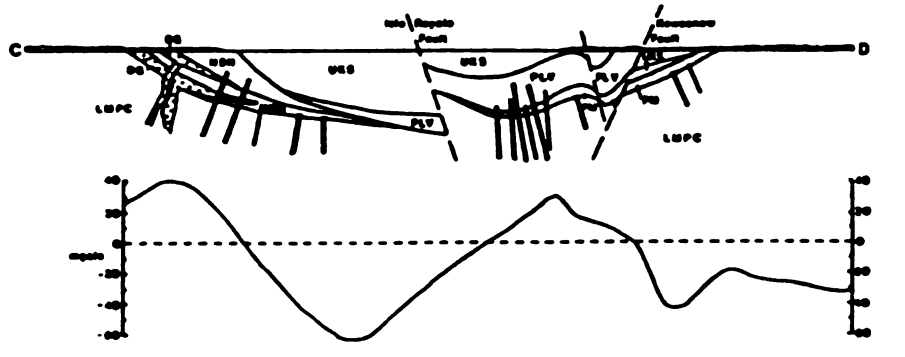

Figure 10. (from Green, 1982). Generalized interpretive geological cross section through figure 8 along CD, with associated Bouger gravity anomaly (use Figure 9 key).

An overall basinward thickening is attributed to the flows and sediments within the rift. Rates of thickening are based on a uniform decrease in dip with distance towards the center (White, 1966), being thickest directly over the basin axis.

Tectonic Models:

There are four basic deformational models which might describe the tectonic origin of the Mid-continent Rift system.

1) Separation of a northern "Minnesota" plate from a southern "Wisconsin" plate about a pole of rotation located at 36° North Latitude, 107° West Longitude, with a separation of 2.6° (Chase and Gilmer, 1973). This model was calculated using rift width measurements taken from the geophysical anomaly and orientations of inferred transform faults and proposes at least 40 km of rifting in Kansas, 65 km under Minneapolis, and 85 km in central Lake Superior.

2) A triple junction with a failed third arm or aulacogen extending northwards. The two southern arms are well defined geophysically, but there are four possibilities for the third, which are shown in Figure 11. The Kapuskasing structural zone trends North-north-easterly from the Lake Superior region and consists of uplifted gneisses and granulites with associated nepheline carbonatite complexes (Watson, 1980, and Van Schumas and Hinze, 1985). The Coldwell Alkaline Province, a series of alkaline intrusions into the Canadian Shield trends almost due north from Lake Superior. The Sibley and Osler Groups, sedimentary packages, dated at 1.35 Ga, trend north-north-west. Trending to the north-west are the North Shore Volcanics and the Duluth complex, which Van Shumas and Hinze, and others consider to be part of the main rift; one of the successful arms.

Around the Lake Superior region there are three groups of dike swarms, the Baraga swarm, the Pukaskwa swarm and the Thunder Bay/Gunflint/Grand Portage swarms, which generally parallel the shoreline. Michell and Platt, (1978), indicate

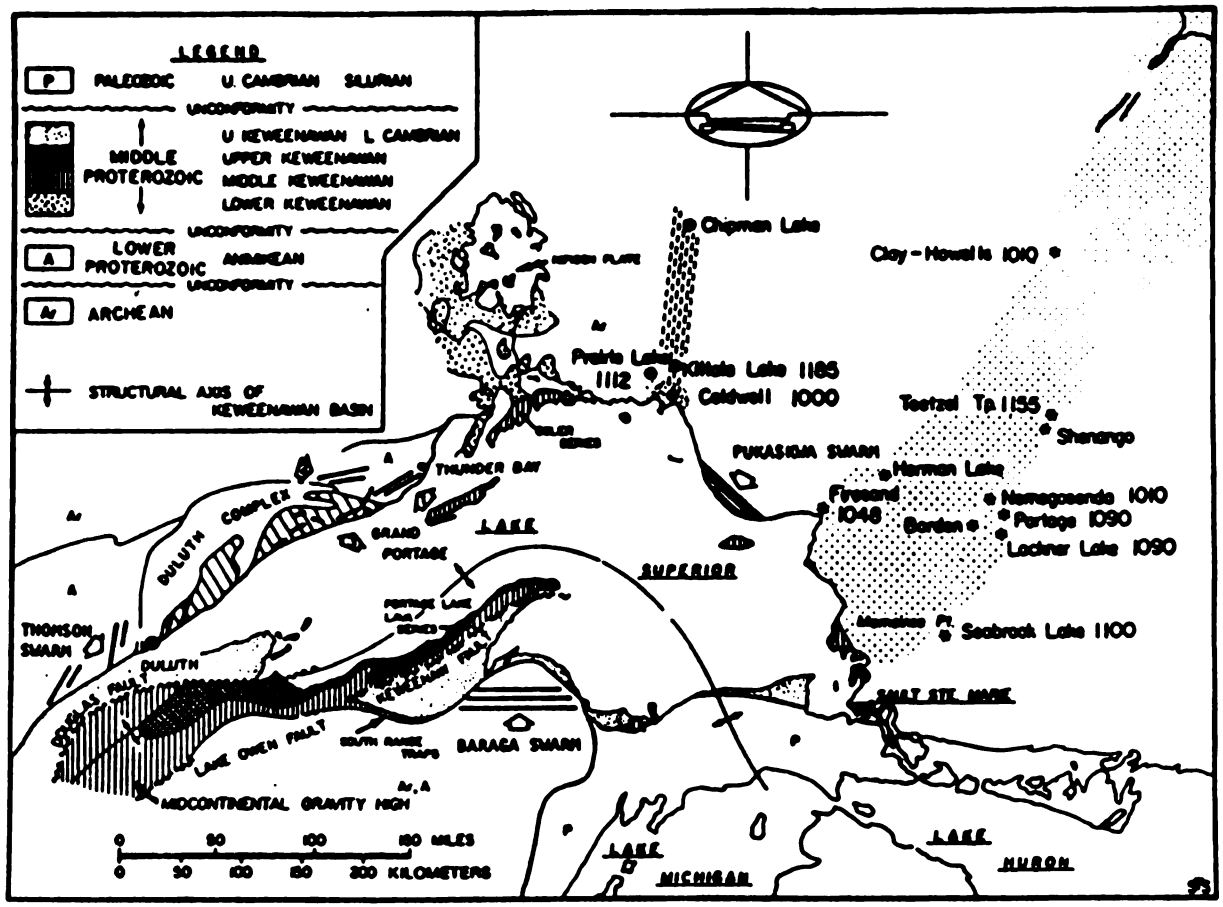

Figure 11. (from Weiblen, 1982). Geological map of Lake Superior region showing possibilities for a failed third arm of a triple junction rift geometry.

these dike swarm orientations are consistent with zones of weakness generated in a hot spot geometry.

3) Impactogen origin (Gordon and Hempton, 1986) in response to the incoming Grenville front. Collisional strain resulted in a series of north-west trending strike slip faults, with left lateral motion and left stepping pattern. This creates a series of trans-tensional pull apart basins. The eventual geophysical pattern seen on magnetic and gravity maps results from the arrangement of the discontinuous basins.

4) Sheared origin (Weiblen, 1982). Weiblen proposed that orientations of the two main rift segments resemble fractures/tension gashes produced in Reidel shear experiments. In these, primary shears form at high angles to the shear couple, then progressively rotate to lower angles, to be more parallel to the shear couple. Conjugate secondary shears again form at high angles, and repeat the rotation process. This model suggests that the two arms of the rift are actually tension gashes with the south east - north west limb having been rotated into the orientation of the shear couple, while the south west - north east limb remained at a high angle.

Regardless of the mode of extension, folding of the units (see Figure 12c & 12d); must have been accomplished by either of, or a combination of the following: 1) Subsidence of the central portion of the rifting area, tilting the originally horizontal units towards the axis of the rift. 2) Compression of the lavas, and interflow sediments, due to a later, superimposed compressional stress. 3) Tilting of the package during the normal faulting associated with rifting (see Figure 12a & 12b and Figure 13). This could occur on large listric faults which have a rotational sense of motion, and not deform the units in any way internally.

The deformation mechanism of the Keweenawan succession might be determined by examining the strain recorded by natural markers in the rocks. If folding did occur, finite strain which can be measured would be imposed on the rock. If the area has not been compressed, but subjected only to extension, as in the second

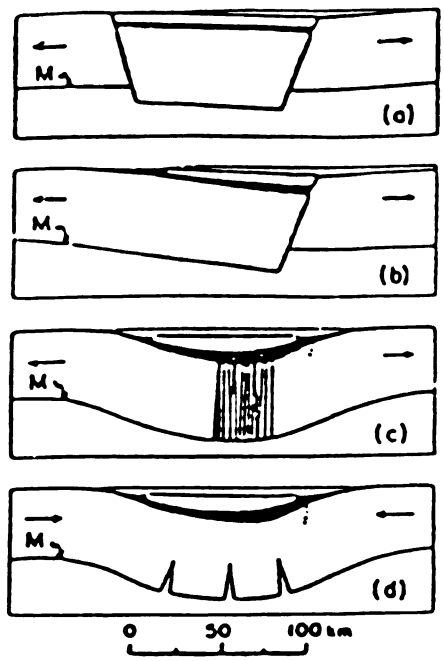

Figure 12. (from White, 1965). Interpreted tectonic models for crustal structure in the Midcontinent Rift.

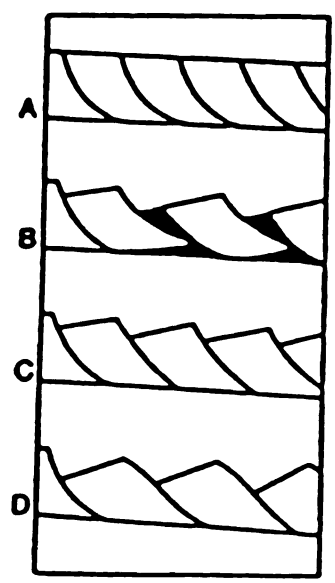

Figure 13. Interpreted tectonic model for crustal structure in the Midcontinent Rift.

case, there would be a noticeable absence of tectonic strain recorded in the rock, except for the simple tilting and the presence of fault planes. From field examinations most the rocks do not appear to have undergone any homogenous flattening which would be associated with folding. The exception to this is the Bohemia conglomerate and other unnamed conglomerates which exist in the deepest exposed section on the peninsula. These rocks do show an apparent fabric to the unaided eye. Visual observations indicate the strain is small, and no precise orientation is indicated, other than an assumed high angle intersection of the compression axis with the synclinal axis.

Large scale normal fault planes do not extend to the surface, which discredits a purely extensional explanation. If these faults are present in the Keweenawan and pre-Keweenawan rocks they are assumed to be buried under post-faulting sediment. The two bounding reverse faults, the Isle Royal/Douglas and the Keweenaw faults, could be explained as reactivated normal faults, which may or may not have extended to the surface before reactivation.

Compressional forces should result in a preferred orientation for pressure solution. In a typical synclinal structure, stress oriented perpendicular to the fold axis would tend to remove more material at grain contacts in this direction. Furthermore, this process should be more evident in the deeper, and hence hotter, interflow conglomerates of the Keweenawan pile. Examinations of thin sections and slabs of these rocks indicate only small amounts of pressure solution have taken place, and not in a consistent fashion. Irregular grain boundaries prohibit volume-loss assumptions in thin section. Hand samples and outcrops do show instances of pressure solution pits on the surfaces of pebbles and cobbles. These are apparent in both the deep rocks from the near the south shore of the penninsula as well as the more shallow north shore rocks.

Figure 13 depicts a tilted portion of the crust (a) which undergoes extension and allows intrusion from below in (b). This results in an overall thinned crust along

normal or listric faults. Although this model does explain the apparent dips observed in the Lake Superior Syncline without compression, it does not explain the presence of the bordering thrust faults.

Figure 12a depicts a classic central graben rift valley. As a result of horizontal tensional stresses the normal-fault-bounded central block is down dropped. Mafic lavas then migrate up the fault planes and flow into the graben followed by sedimentation of detritus eroded from the adjacent scarps and flows. Figure 12b is the same model with a half graben depicted which aids in creating the observed asymmetric dip. This model adequately accounts for crustal thickening with a classic rift crustal structure. However it has been pointed out (White, 1965) that the major source for sediment are the flows themselves and not the material which would be exposed in a fault scarp. The units may be made to dip inward by progressive subsidence of the fault block; each bed is deposited horizontally and then tilted during basin downdrop. This model does not, at all, explain the presumed uplift along the Keweenaw and Douglas faults without invoking a completely separate compressional phase.

Figure 12c shows a crustal tension which does not result in normal faulting but tensional fractures through the crust. These fractures allow intrusion of dike swarms into the crust which then subsides isostatically from the increased load. Lava flows and sedimentary units fill in the downwarped basin. This then becomes a self-perpetuating rift; the subsidence causes further fracturing allowing more intrusion, which creates more subsidence. This model is most attractive geophysically because it it accounts for the high density/high velocity material at depth, while explaining the observed dips of the rock units (White, 1965). Again, it falls short of explaining the central uplift along thrust faults relative to the margins of the rift zone, without a separate compression.

Figure 12d provides a purely compressional model to account for the observed features. Compressional stresses result in original downwarping which is filled in by sediments at first. The lower half of the crust undergoes extension allowing intrusion

of magmas to shallow depths. Dikes reaching to the surface act as feeders for the lava flows. Crustal loading from sediment and lava continues the downwarp of the crust isostatically, resulting in postrift stratigraphic onlap. These two phases of downwarping result in a classic "steer's head" geometry as seen in other rift systems (White and McKenzie, 1988). After compressional forces are eased, isostatic equilibrium is restored by central uplift (White, 1965), or alternatively, the compression results in thrusting on the margins of the basin, and the sediment/flow package rides up as the "vise" of country rock closes. This model adequately explains geologic and geophysical features, but it is questionable whether it allows for the massive outpouring of lavas observed or the regional slope of the whole MRS anomaly.

Methods:

To help constrain which of the models of deformation is more applicable to the Mid-Continent Rift system, I measured the recorded strain in some of the Keweenawan rocks. The orientation and amount of strain indicate the pattern of tectonic stresses for a given area, and either support or refute the various deformational models.

The two main Keweenawan rock types exposed in the study area are conglomerates and basaltic lavas (see Figure 14). The lavas are a more homogenous rock, and although they must have recorded strain, there are no apparent markers available to measure. Conglomerates are the better candidate for recording strain because they contain good markers in the form of pebbles and cobbles. Furthermore, the older, and therefore originally deeper conglomeratic units should have recorded the most strain. The most prominent unit is the Bohemia Conglomerate which is the deepest, continuous inter-flow sedimentary unit exposed in the area. Samples from two other unnamed inter-flow conglomerate/sands were also collected. These came from slightly deeper sections of the lava/sediment pile, and were steeper dipping than the Bohemia samples.

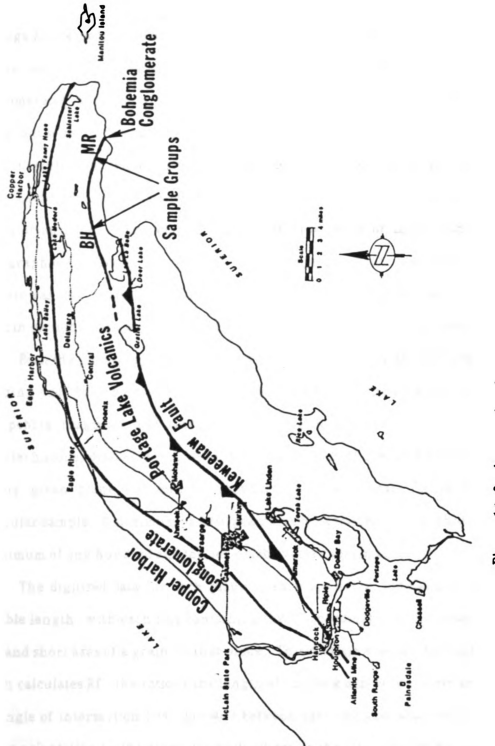

Figure 14. Study area showing sample groupings.

The collected samples are red to brown, predominantly sandy, pebble conglomerates, the sand portion consisting of lithic fragments having the same lithology as the pebbles. The clasts are rounded to well rounded felsic volcanics, with smaller amounts of mafic and intermediate volcanics present as well. Both conglomerates and sands are cemented, predominantly with coarsely crystalline calcite, but some silica and ferric oxide are present also.

Oriented specimens were collected from various conglomeratic outcrops in the field. Each specimen was then cut along three mutually perpendicular planes of known orientation. Thin sections were made from each of these planes, and then photographed. In two of the samples, the average grain size was large enough that analysis was also carried out on transparent overlays of the three planes in slab form, and thin sections were made out of a finer grained fraction of the specimen.

Both the photographs and overlays were digitized using an IBM PC with attached digitizing pad. Four points representing the endpoints of the long and short axis for each pebble, fragment, and sand grain were digitized into an XY coordinate system, using techniques discussed in Lisle (1984). The number of grains which were digitized on any given plane was directly dependent on the average grain size for that particular sample. A minimum of fifty grains were examined for the thin sections and a maximum of one hundred and ten for a slab overlay specimen.

The digitized data for each plane of each specimen consisted of a datafile of variable length, with each line containing the XY coordinates of the endpoints for the long and short axes of a grain in that plane. This datafile was run through a program which calculates Rf - the ratio of the length of the long axis to the short axis, and Phi - the angle of intersection (-90° to +90°) between the long axis and a reference line of known orientation on the plane, for each ellipse in the file. The Rf/Phi data produced a vector mean Phi, and a harmonic mean Rf, when run through a symmetry analysis

program. The vector mean Phi orientation represents the elongation direction in that particular plane, and Rf a measure of that elongation.

The next step is to calculate the strain ellipsoid values. TRYELL is a program which receives all the data: mean Rf/Phi, number of planes per sample and their orientaion, as well as a weighting value, then the program yields trial strain ellipsoid axes lengths and orientations. In all of this study's samples, each plane was weighted equally, as all measurements were of equal accuracy and every plane, for any given specimen, had the same number of elliptical markers.

The data output from TRYELL is then entered into BESTELL, which completes a series of iterations, yielding a best fit ellipsoid. These data are shown and explained further in Appendix A. A maximum of five iterations is done for each of cell of the strain matrix. If the solution for one iteration is identical to the previous one, the calculations stop. Thus some samples have more data points for strain axes than others.

Results:

The primary data plot for this project is the lower hemisphere, equal area stereo net projection, otherwise known the Schmidt net. On the Figures 15 through 27 are the various stereo plots of the BESTELL data. The left hand plot for each sample shows the positions of the X (long) axis locations from the BESTELL iterations with a square symbol, Y (intermediate) axis positions with a triangle, and Z (short) axis with a cross. The right hand plot is the same specimen data with the structural dip rotated back to horizontal.

Table 1 shows the mean strain axes lengths for each sample measured and the average strain for that entire region. The average value depicts a situation which has undergone nearly pure plane strain simple shear, where $X > Y=1 > Z$. The values are not perfect for the case of plane strain; Y is not precisely equal to 1.000, and shortening in Z does not exactly compensate for elongation in X.

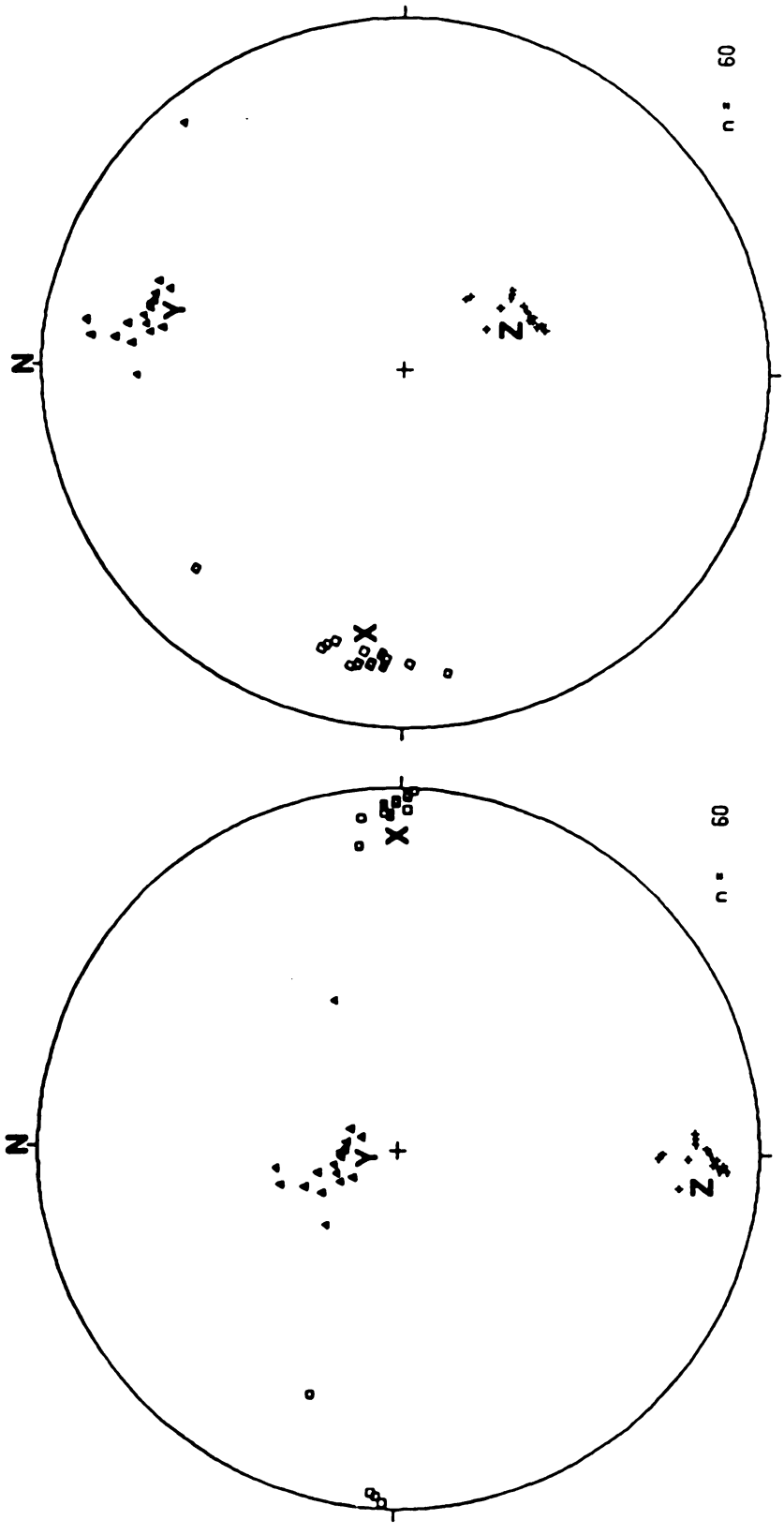

Figure 15. Stereo net plot of sample MR1. Left hand plot is of strain axes as they are in outcrop. Right hand plot has had structural dip removed by rotating -54° around 295, 00.

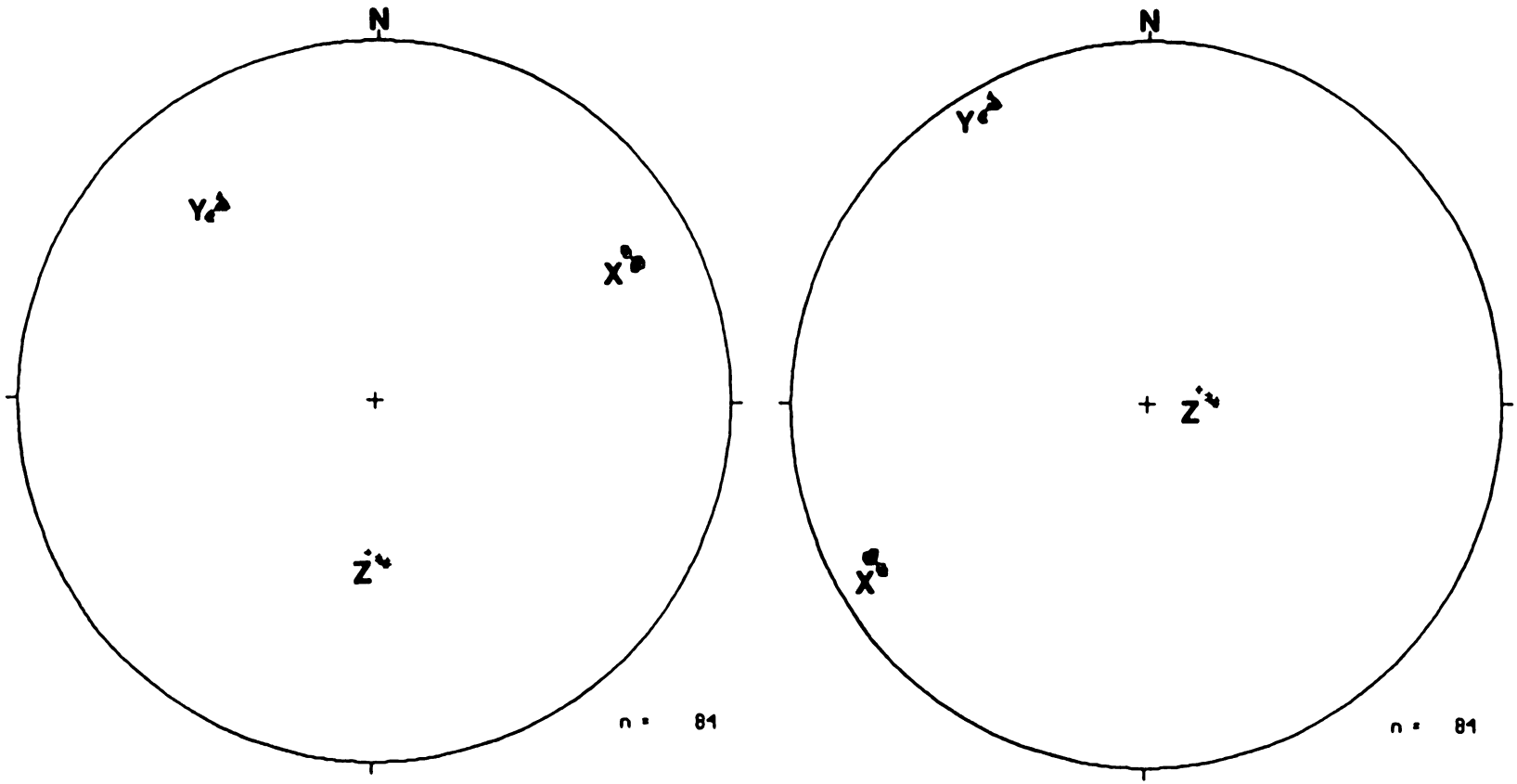

Figure 16. Stereo net plot of sample MR2. Left hand plot is of strain axes as they are in outcrop. Right hand plot has had structural dip removed by rotating -41° around 290°, 00°.

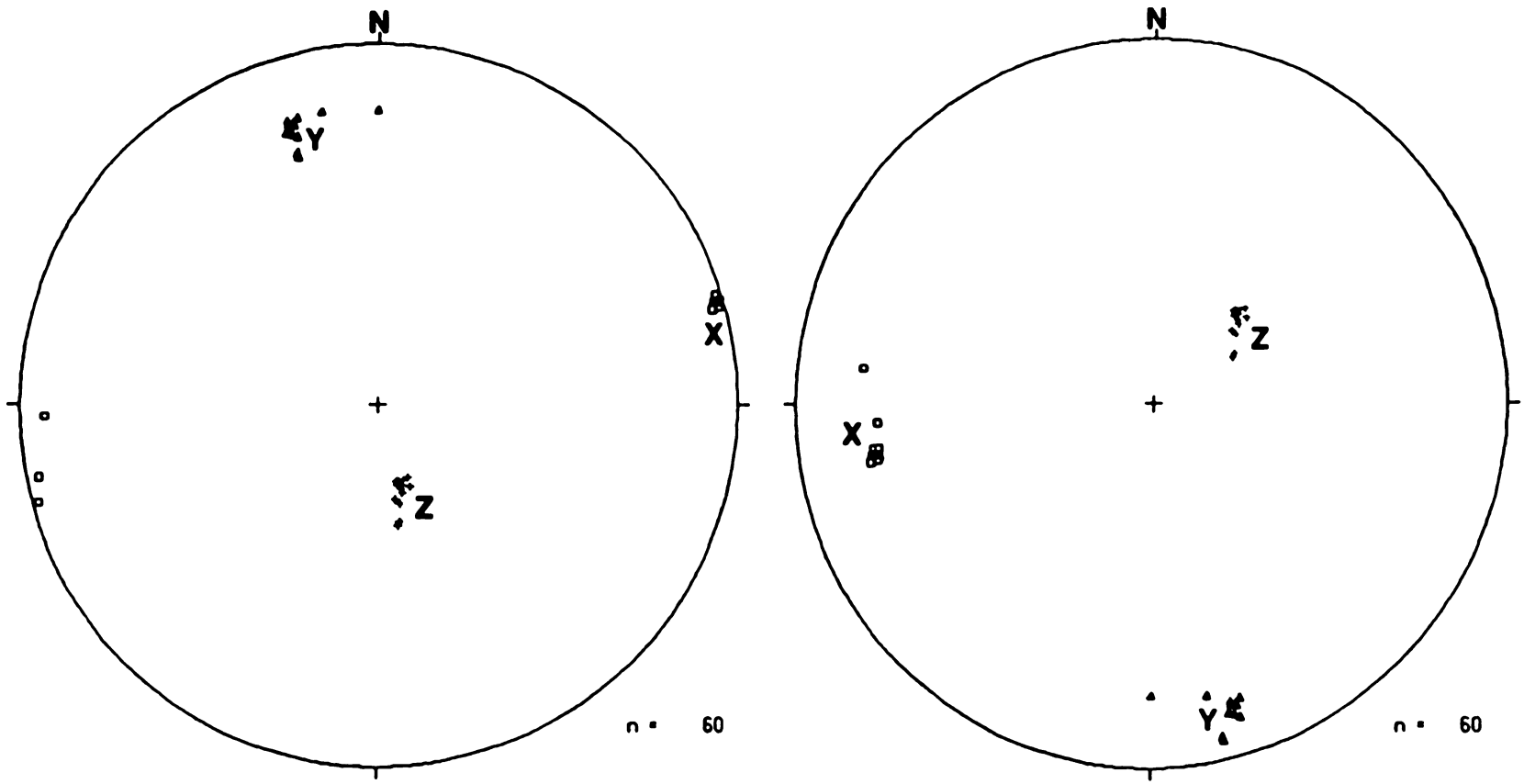

Figure 17. Stereo net plot of sample MR2SL. Left hand plot is of strain axes as they are in outcrop. Right hand plot has had structural dip removed by rotating -41° around 290°, 00°.

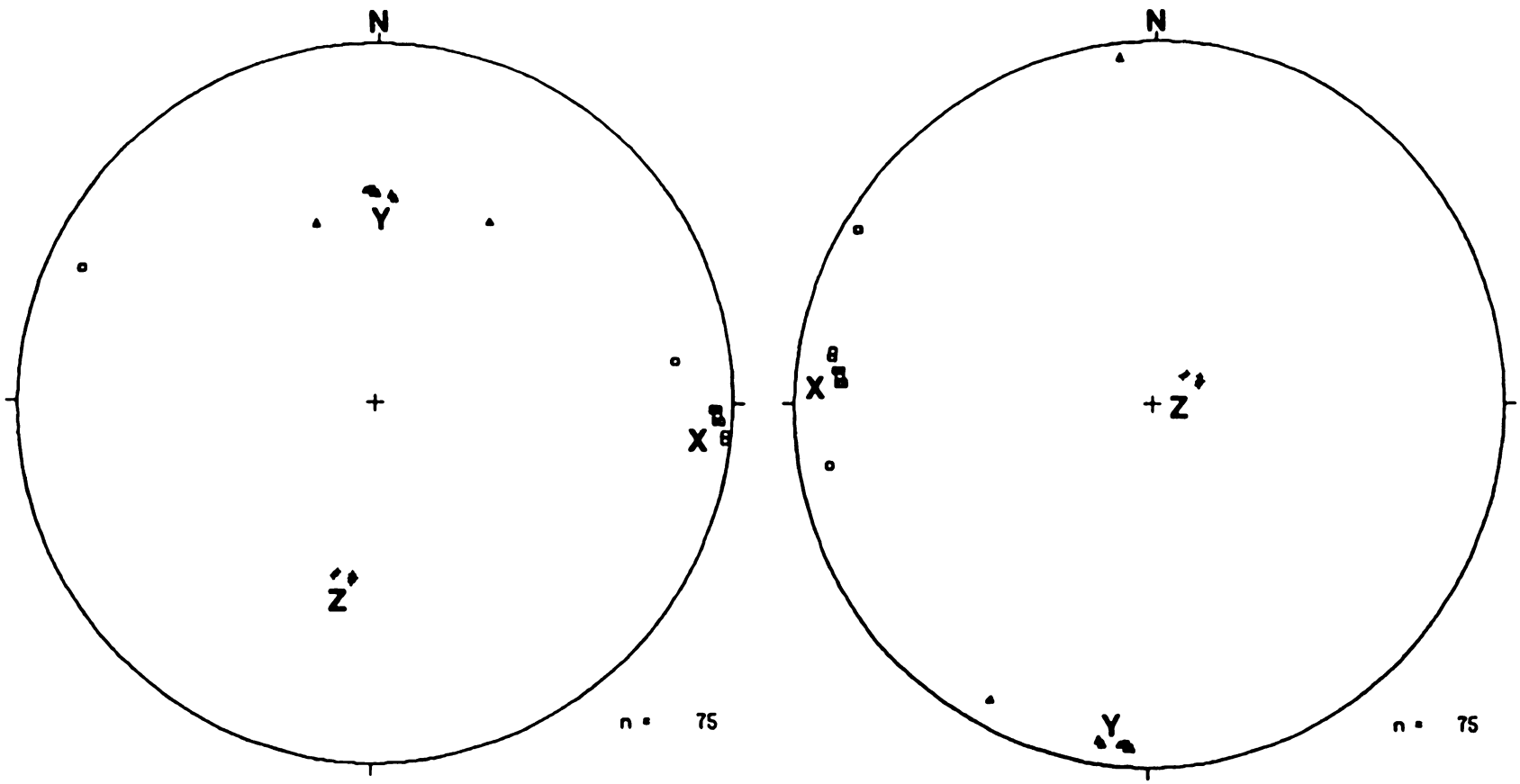

Figure 18. Stereo net plot of sample MR3. Left hand plot is of strain axes as they are in outcrop. Right hand plot has had structural dip removed by rotating -49° around 290°, 00°.

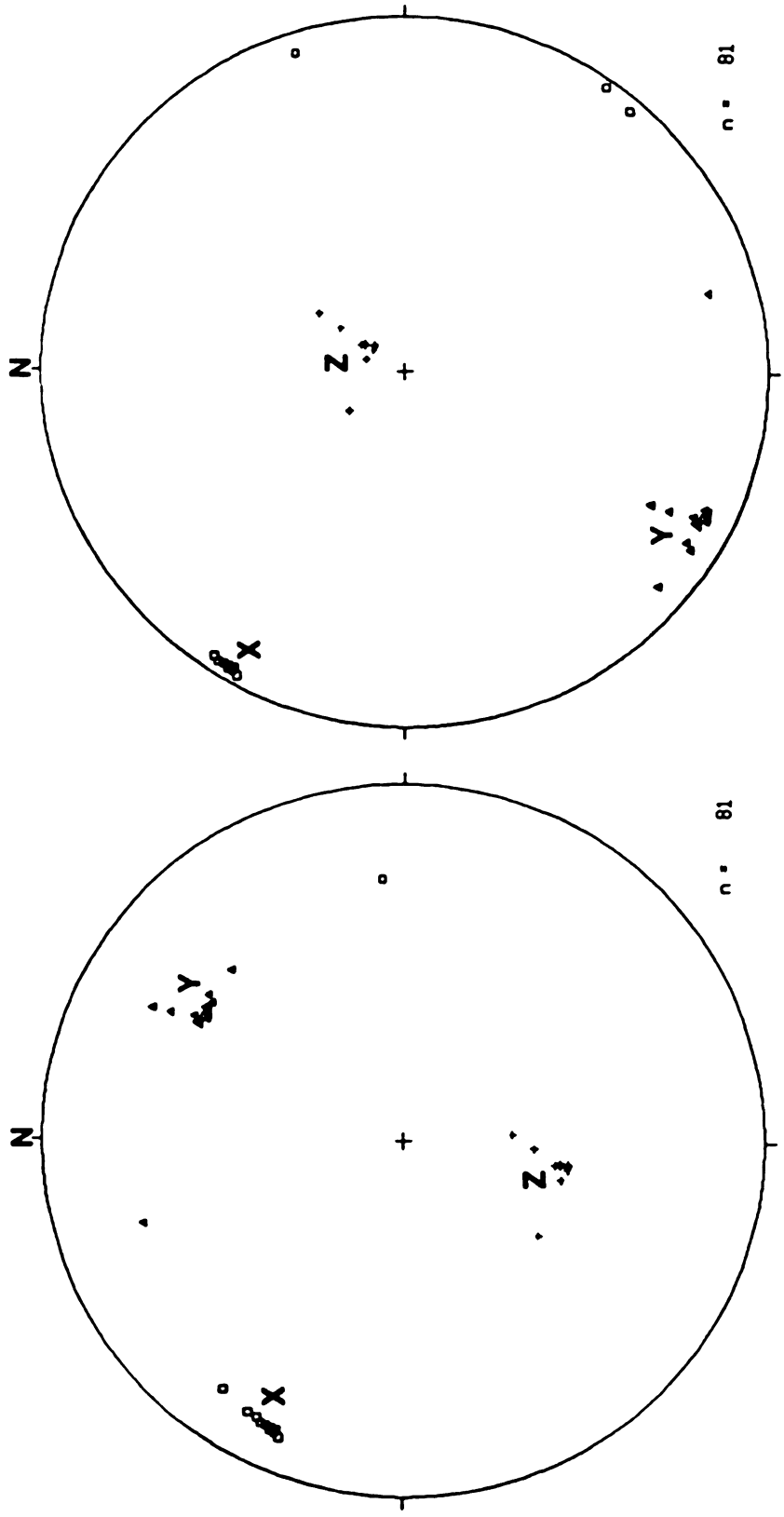

Figure 19. Stereo net plot of sample MR9. Left hand plot is of strain axes as they are in outcrop. Right hand plot has had structural dip removed by rotating -46° around 285°, 00°.

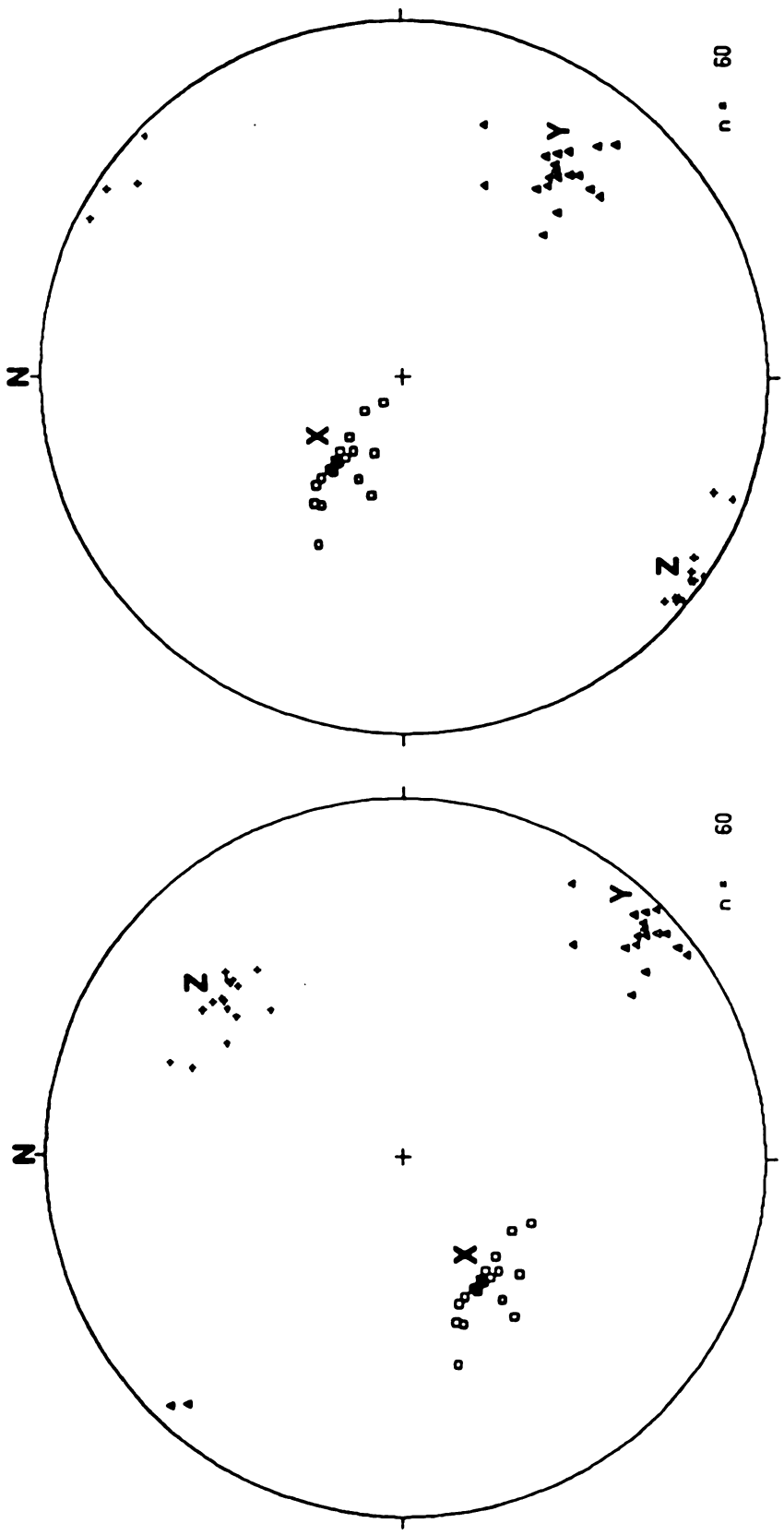

Figure 20. Stereo net plot of sample MR10. Left hand plot is of strain axes as they are in outcrop. Right hand plot has had structural dip removed by rotating -40° around 280°,00°.

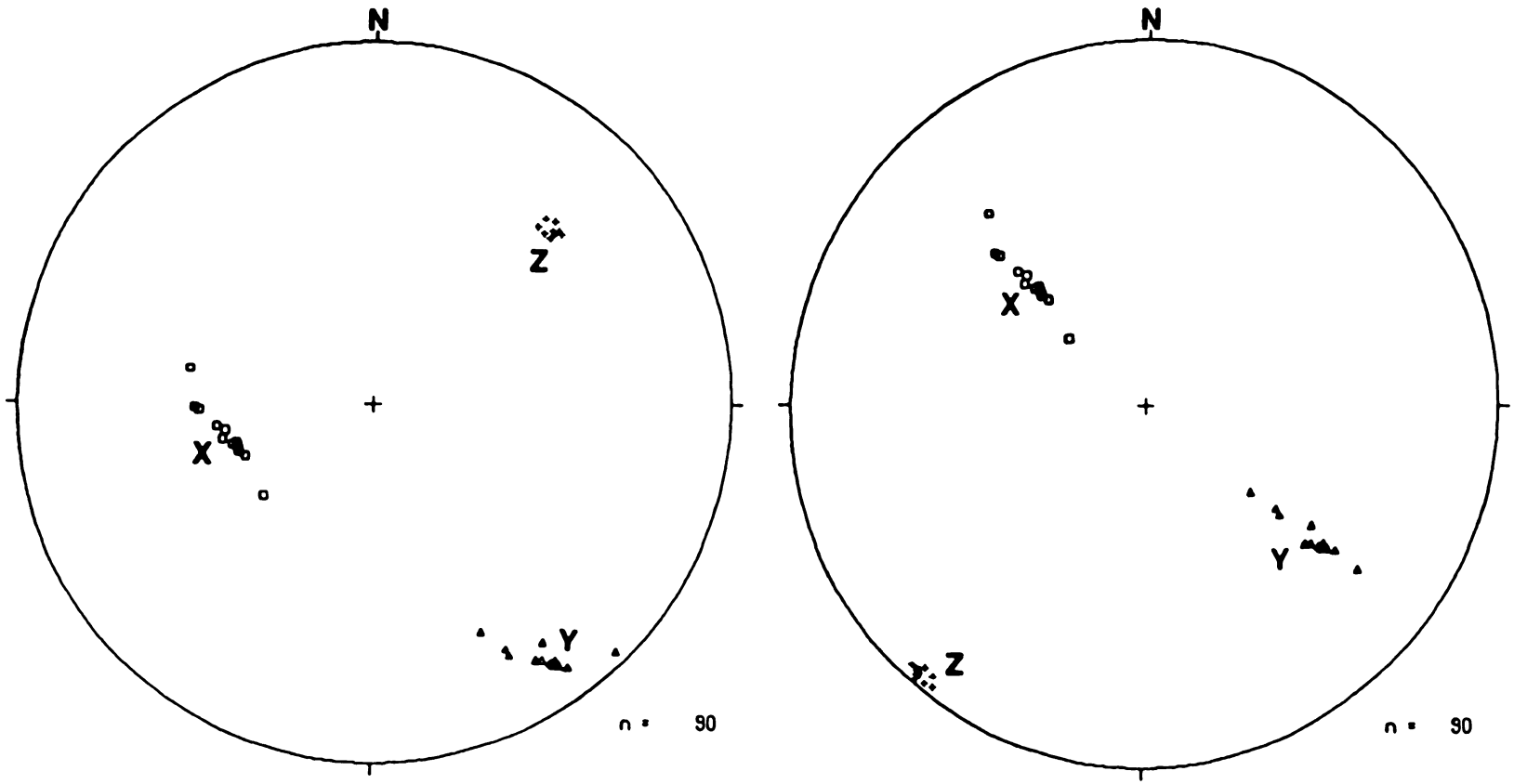

Figure 21. Stereo net plot of sample MR10SL. Left hand plot is of strain axes as they are in outcrop. Right hand plot has had structural dip removed by rotating -40° around 280°, 00°.

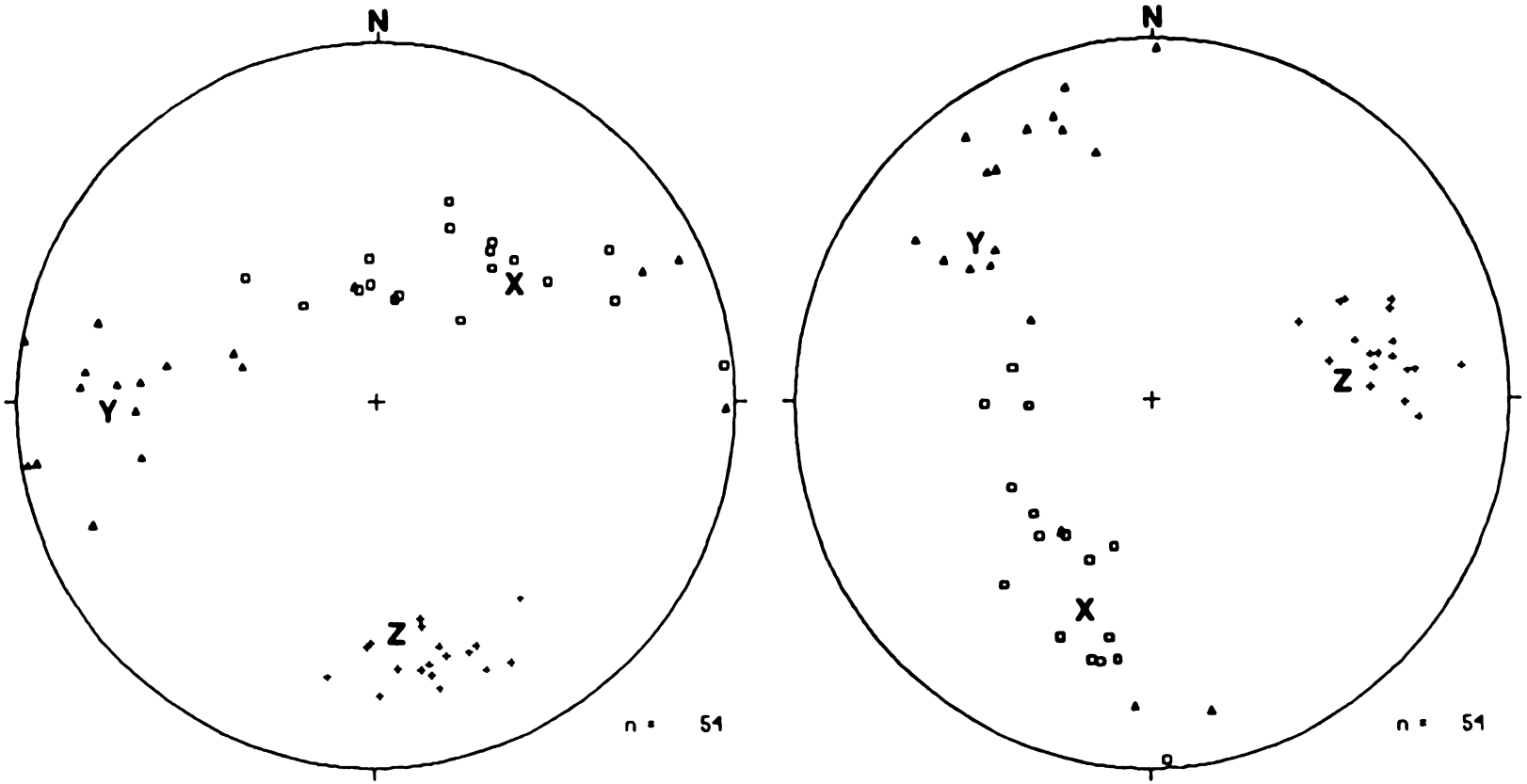

Figure 22. Stereo net plot of sample PU1. Left hand plot is of strain axes as they are in outcrop. Right hand plot has had structural dip removed by rotating -99° around 301°, 00°.

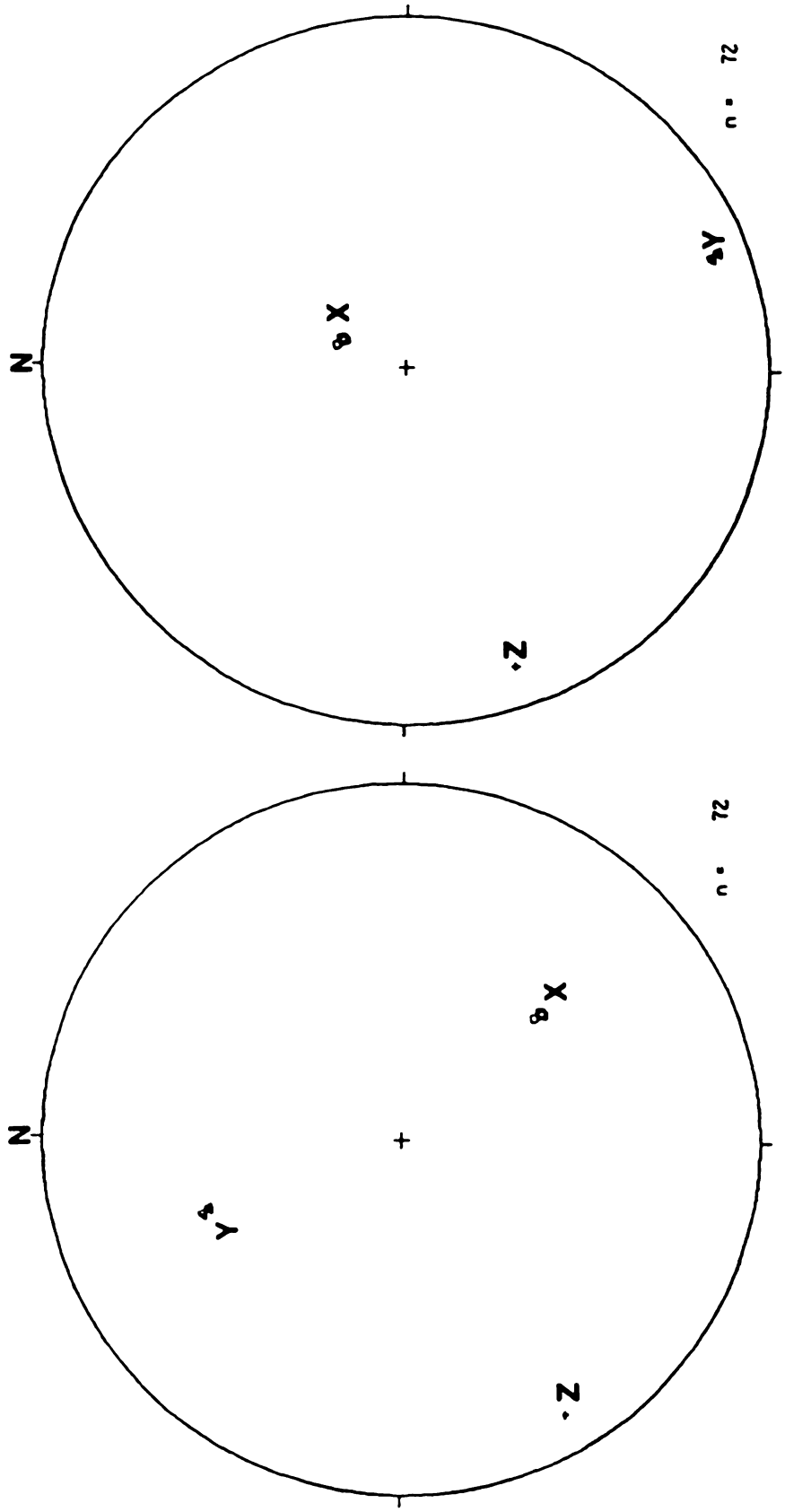

Figure 23. Stereo net plot of sample BH1. Left hand plot is of strain axes as they are in outcrop. Right hand plot has had structural dip removed by rotating 51° around 065°,00°.

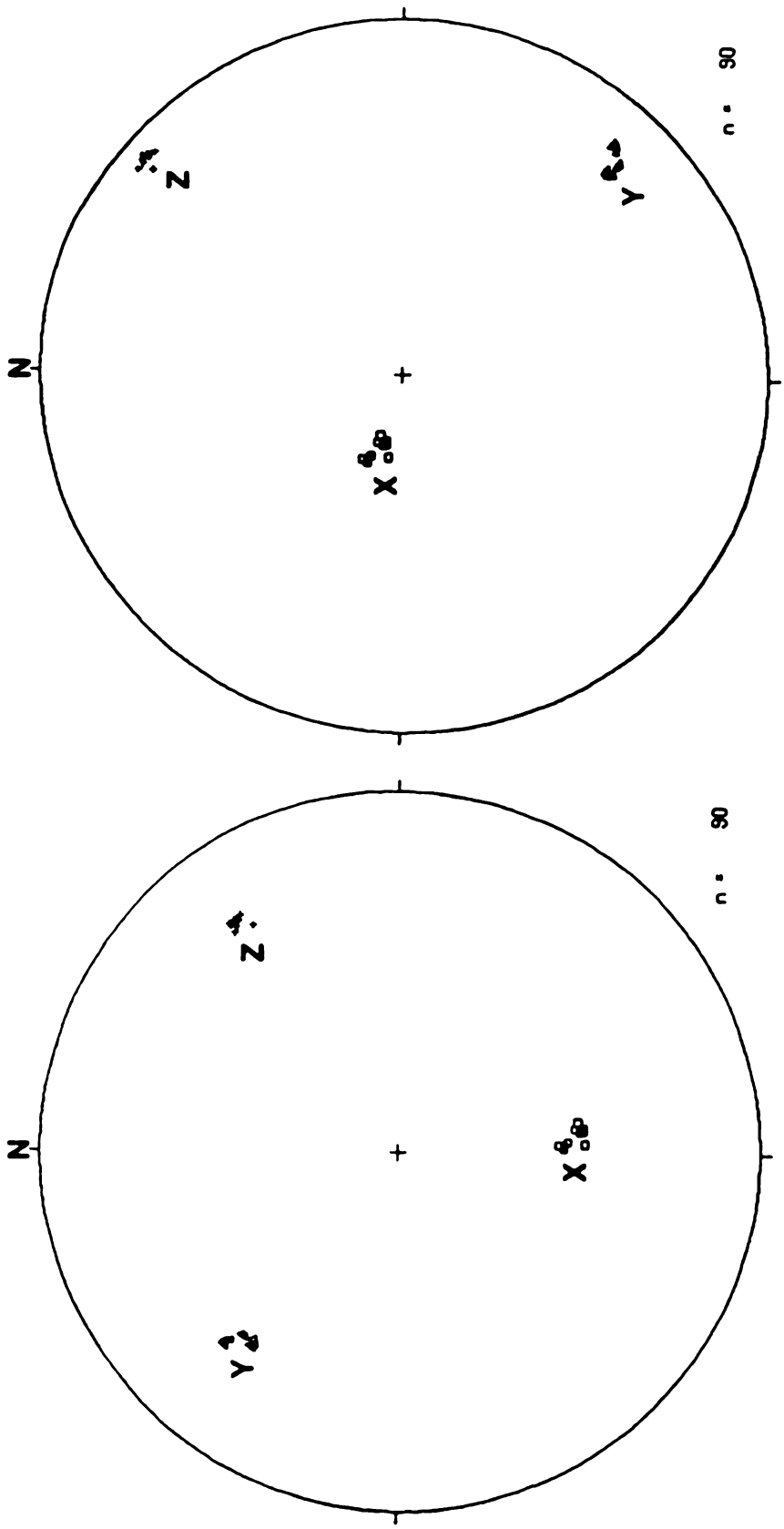

Figure 24. Stereo net plot of sample BH1SL. Left hand plot is of strain axes as they are in outcrop. Right hand plot has had structural dip removed by rotating 51° around 065°, 00°.

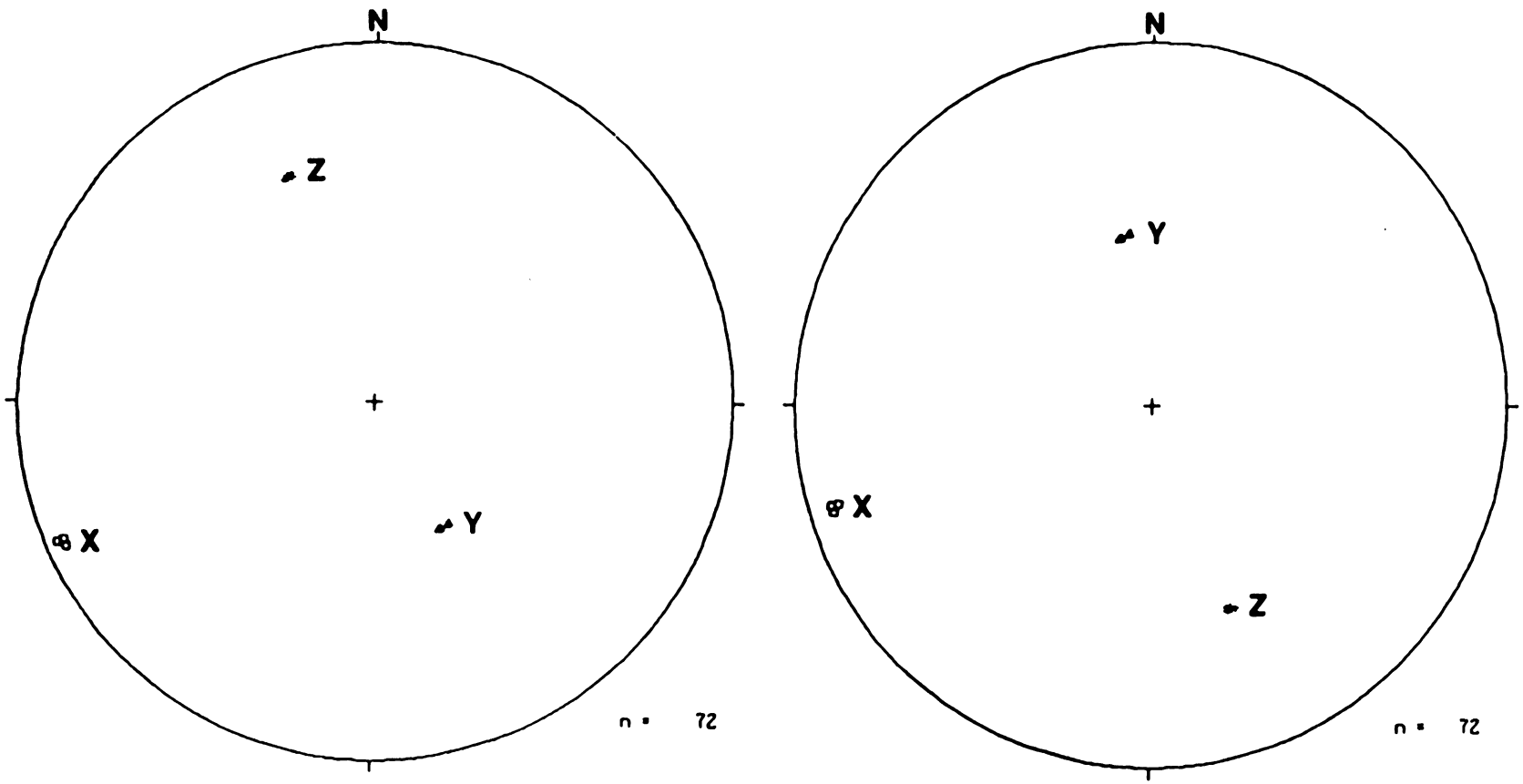

Figure 25. Stereo net plot of sample PL1. Left hand plot is of strain axes as they are in outcrop. Right hand plot has had structural dip removed by rotating 71° around 071°, 00°.

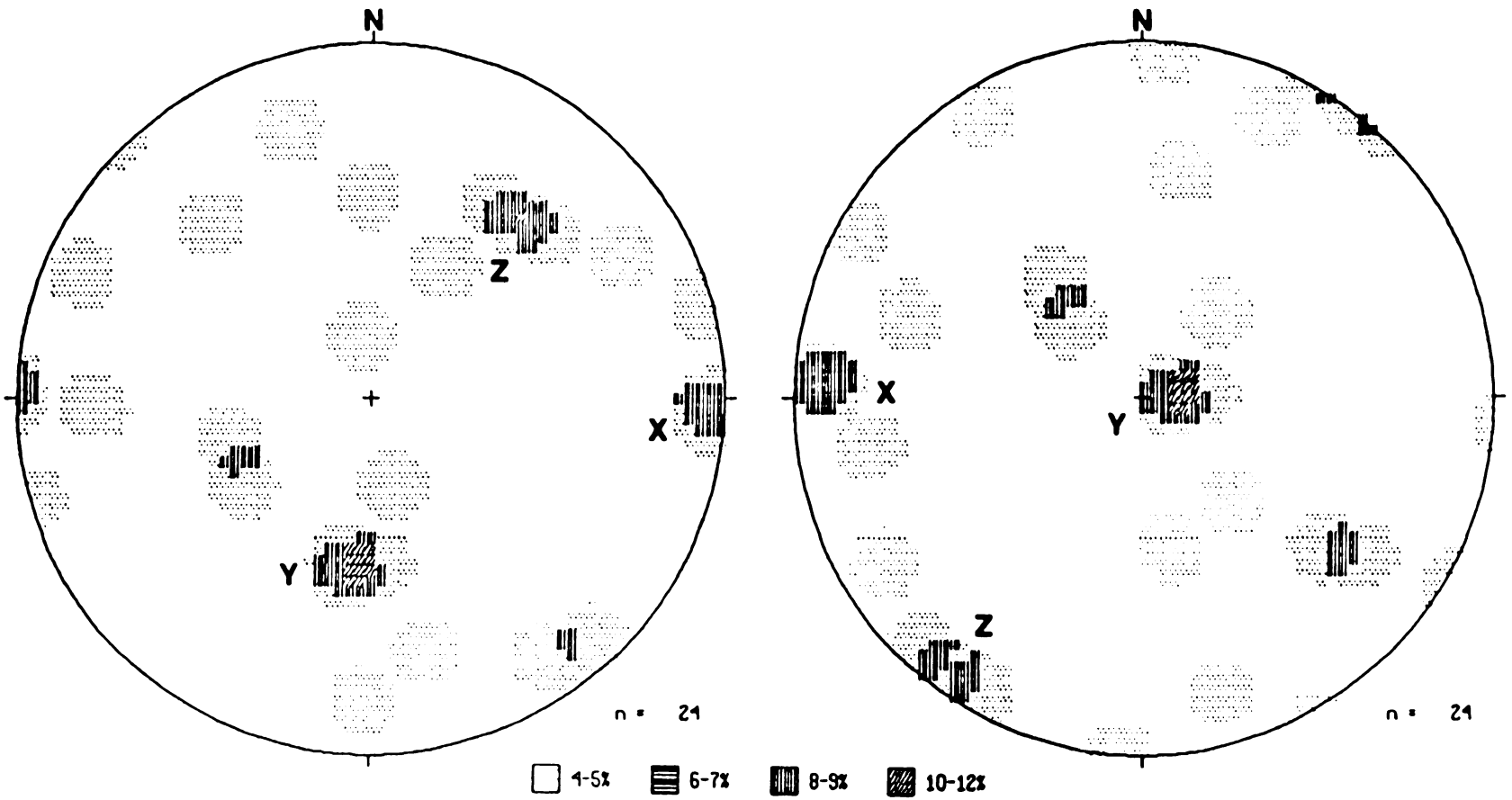

Figure 26. Contoured calculated strain axes (1% area radius) stereo net plot of all "MR" and "PU" samples. Left hand plot is of strain axes as they are in outcrop. Right hand plot has had structural dip removed by rotating -49° (mean dip) around 287°, 00° (mean strike).

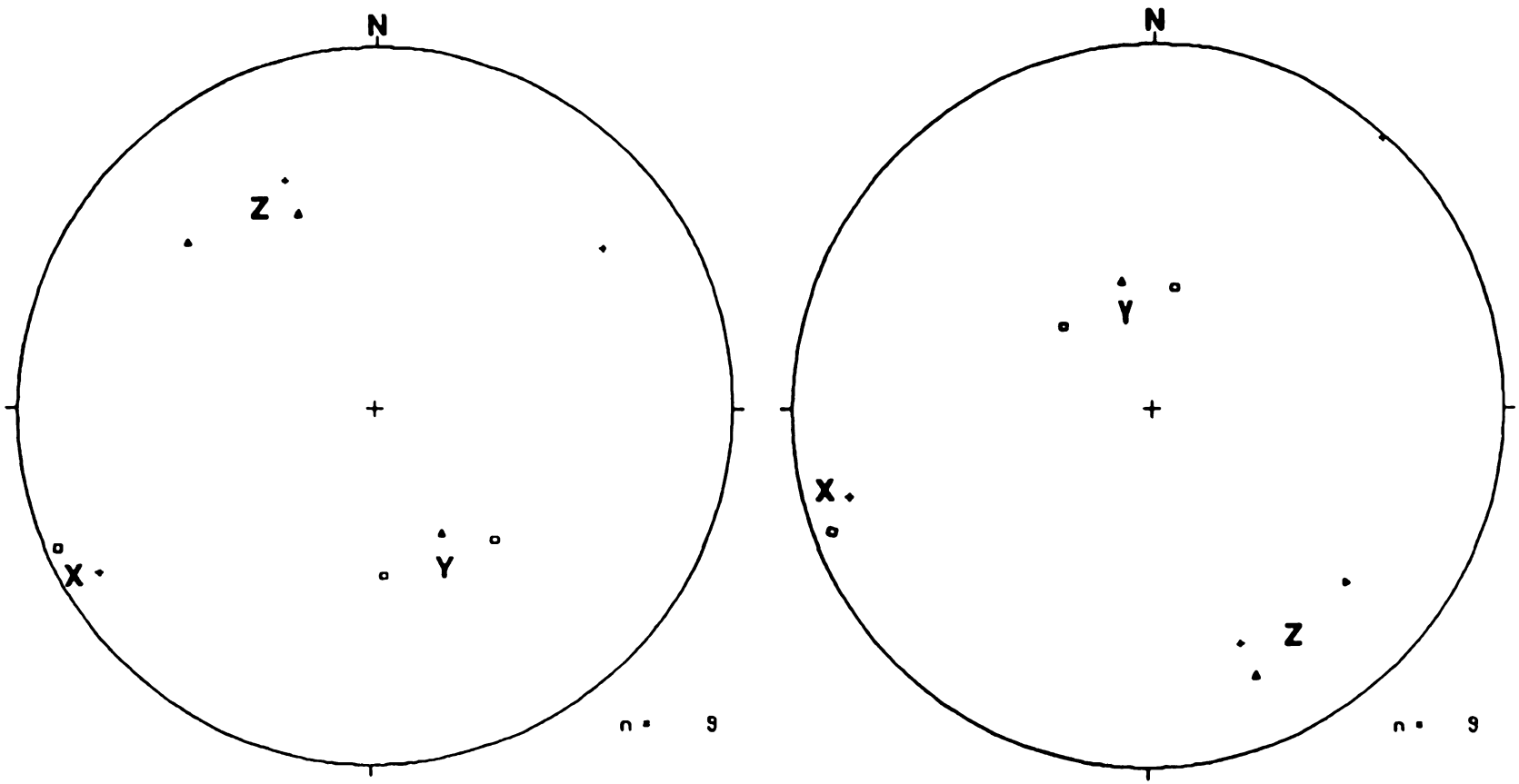

Figure 27. Stereo net plot of samples "BH" and "PL". Left hand plot is of strain axes as they are in outcrop. Right hand plot has had structural dip removed by rotating 57° (mean dip) around 066°, 00° (mean strike).

TABLE 1 Finite strain axis values from samples

Sample	X axis	Y axis	Z axis
MR1	1 655	0 993	0 613
MR2	1 983	0 870	0 580
MR2SL	1 806	0 941	0 592
MR3	1 311	1 110	0 660
MR9	1 548	1 044	0 638
MR10	1 593	1 039	0 612
MR10SL	1 377	1 181	0 615
PU1	1 821	0 982	0 588
BH1	1 763	0 905	0 627
BH1SL	1 816	0 873	0 632
PL1	1 548	1 023	0 631
MEAN	1 656	0 996	0 617

One inconsistancy between samples is the phenomonon of axes changing orientations Although all samples except PU1 and PL1, have an axis which plots near vertical, it is not always the same axis Samples MR1, MR2, MR3 and MR9 have Y near vertical Samples MR10, PU1 and BH1 have an X near vertical The framework of the three mutually perpendicular axes remains reasonably consistent, but the actual axes transpose themselves from one sample to another This an acceptable and expected phenomonon in regions of low stress The markers in each sample are changing shape in response to tectonic stress Because the markers were originally ellipsoidal pebbles, and originally had irregular orientations the pebbles would change shape in different ways A pebble whose long axis corresponded with the elongation direction (vertical), would follow a strain path of continual stretching and its long axis would have a similar post-deformation orientation One whose short axis was vertical and therefore continually stretched, would still have a vertical short axis if deformed only slightly, and yield a vertical Z axis instead of an X axis

It is therefore proposed that the strain ellipsoid for this region is best represented by a near-vertical Y axis plunging steeply south, a near horizontal east-west X axis plunging slightly east, and a Z axis which plunges slightly north This

particular reference frame is shown imposed on the samples in Figures 26 and 27, which correspond to the two distinct sample clusters as shown by Figure 14. As should be expected; for the BH-PL group, the XY plane shows a north-east orientation, and the MR-PU group's XY plane shows a very slight north-west orientation. In both cases, the XY plane is consistent with bedding strike in the respective areas, and the elongation direction is parallel to the Keweenaw Fault.

Such an orientation for the strain axes of this region indicates a compressional tectonic phase was superimposed on the Keweenawan sequence after the extensional phase. Shortening in a north-south direction produced the synclinal characterisitcs of the Lake Superior region. Such a compression also explains the bordering thrust faults. These could either have originated at the time of compression or have been reactivated normal faults (or shallower continuations thereof) related to original extension.

The presence of microfractures in the thin sections supports the argument for compression in a generally north-south direction. These fractures tend to be mineralized with coarsely crystalline calcite and quartz. They are depicted in Figures 28 through 35 as lines within the plane of the three thin sections for each sample. Fractures with a mean orientation of N18E, 87S (nearly vertical) could form as extensional features during loading, with the greatest principal stress oriented horizontally in a north-south direction, and the axis of least principal stress being horizontal in an east-west direction (perpendicular to the fractures).

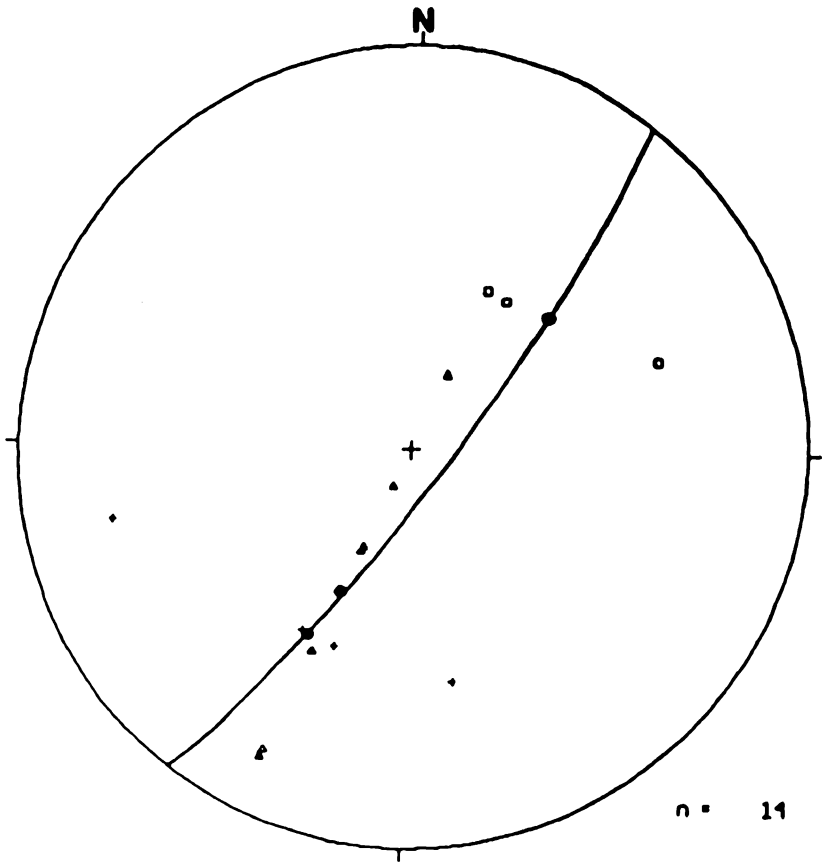

Figure 28. Stereo net plot of fractures from sample MR1. Squares represent fractures on MR1-1, triangles for MR1-2, and crosses for MR1-3. Solid circles are the mean orientations of the fracture traces for each plane. The plotted plane represents best fit plane of fracture.

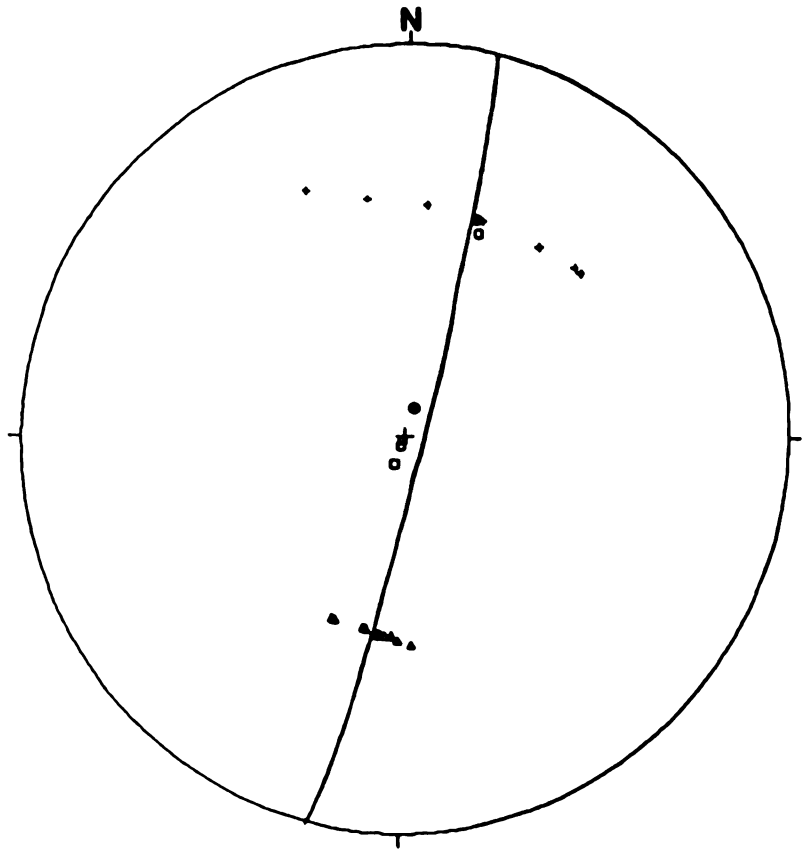

Figure 29. Stereo net plot of fractures from sample MR2. Squares represent fractures on MR2-1, crosses for MR2-2, and triangles for MR2-3. Solid circles are the mean orientations of the fracture traces for each plane. The plotted plane represents best fit plane of fracture.

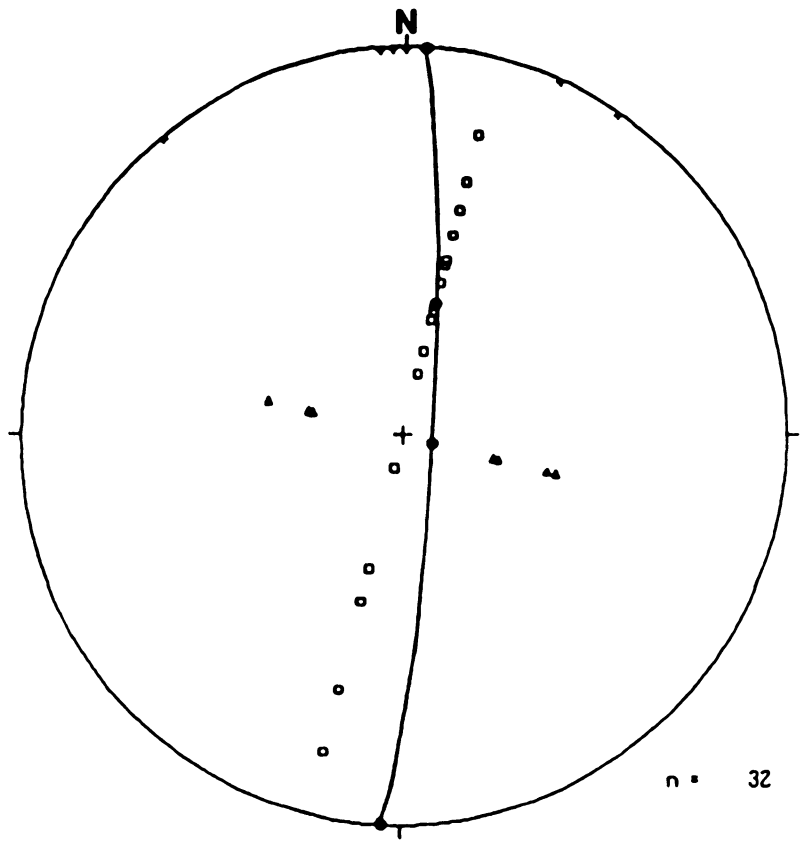

Figure 30. Stereo net plot of fractures from sample MR3. Squares represent fractures on MR3-1, triangles for MR3-2, and crosses for MR3-3. Solid circles are the mean orientations of the fracture traces for each plane. The plotted plane represents best fit plane of fracture.

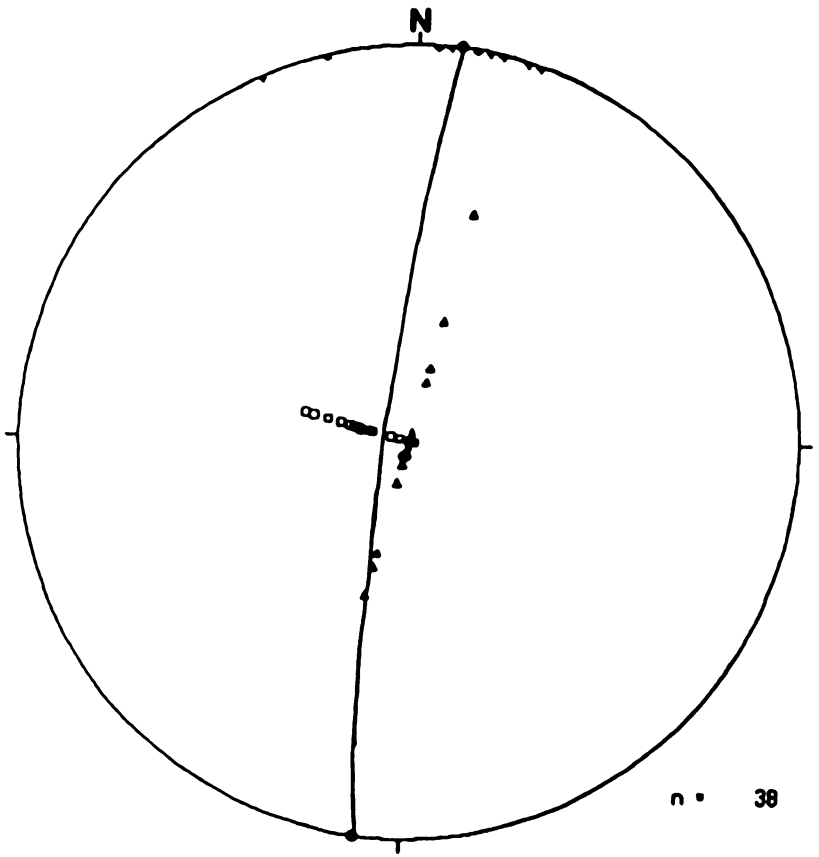

Figure 31. Stereo net plot of fractures from sample MR9. Squares represent fractures on MR9-1, triangles for MR9-2, and crosses for MR9-3. Solid circles are the mean orientations of the fracture traces for each plane. The plotted plane represents best fit plane of fracture.

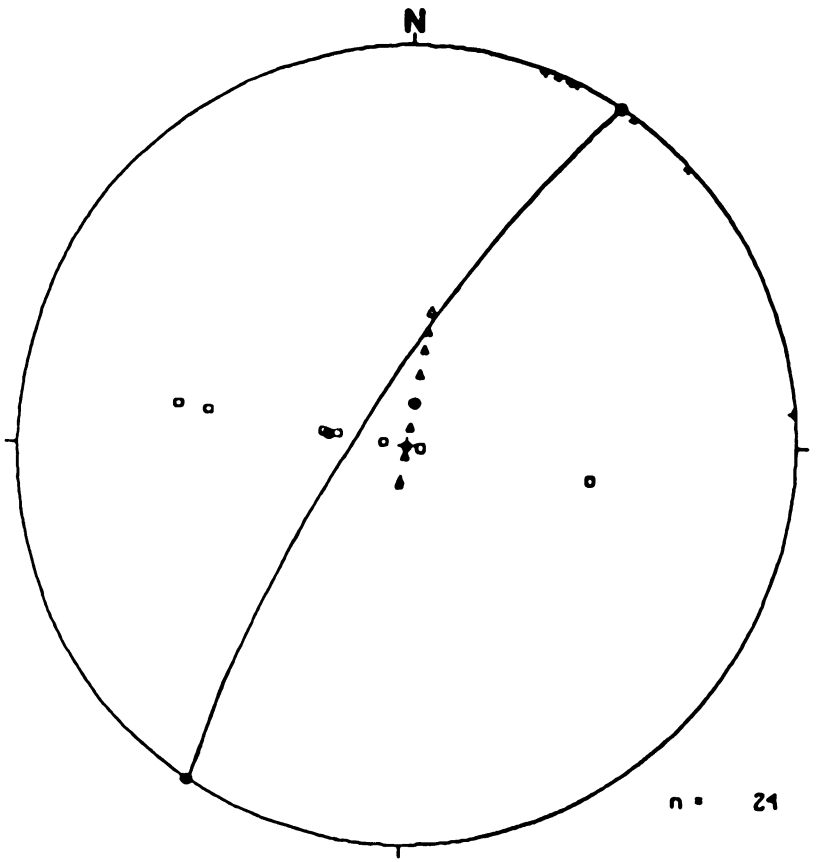

Figure 32. Stereo net plot of fractures from sample MR10. Squares represent fractures on MR10-1, triangles for MR10-2, and crosses for MR10-3. Solid circles are the mean orientations of the fracture traces for each plane. The plotted plane represents best fit plane of fracture.

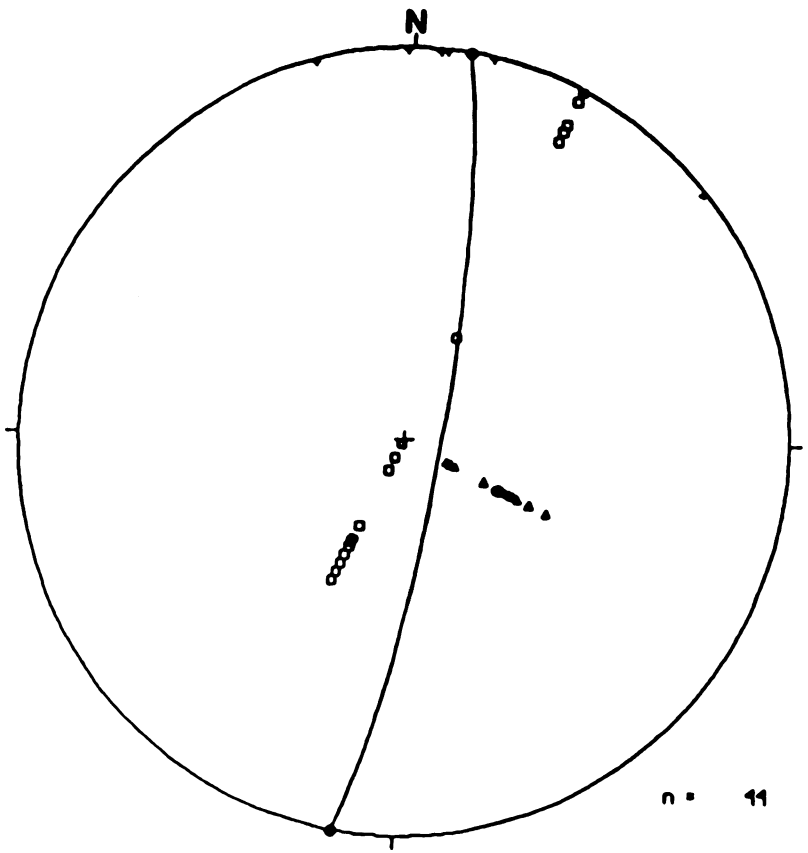

Figure 33. Stereo net plot of fractures from sample PU1. Squares represent fractures on PU1-1, triangles for PU1-2, and crosses for PU1-3. Solid circles are the mean orientations of the fracture traces for each plane. The plotted plane represents best fit plane of fracture.

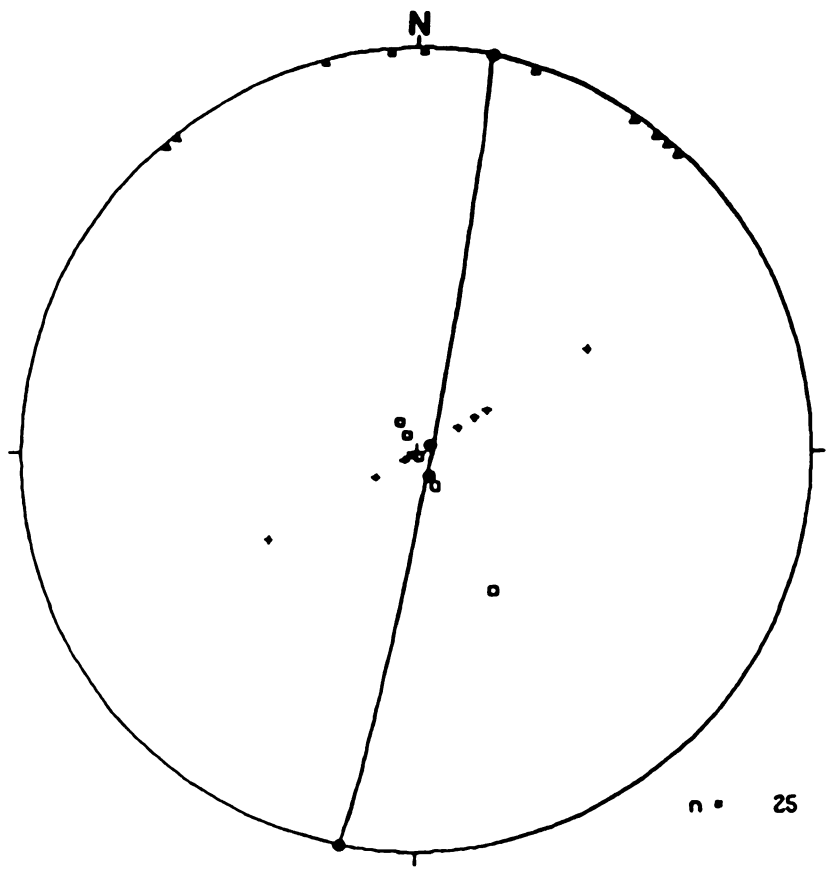

Figure 34. Stereo net plot of fractures from sample BH1. Squares represent fractures on BH1-1, triangles for BH1-2, and crosses for BH1-3. Solid circles are the mean orientations of the fracture traces for each plane. The plotted plane represents best fit plane of fracture.

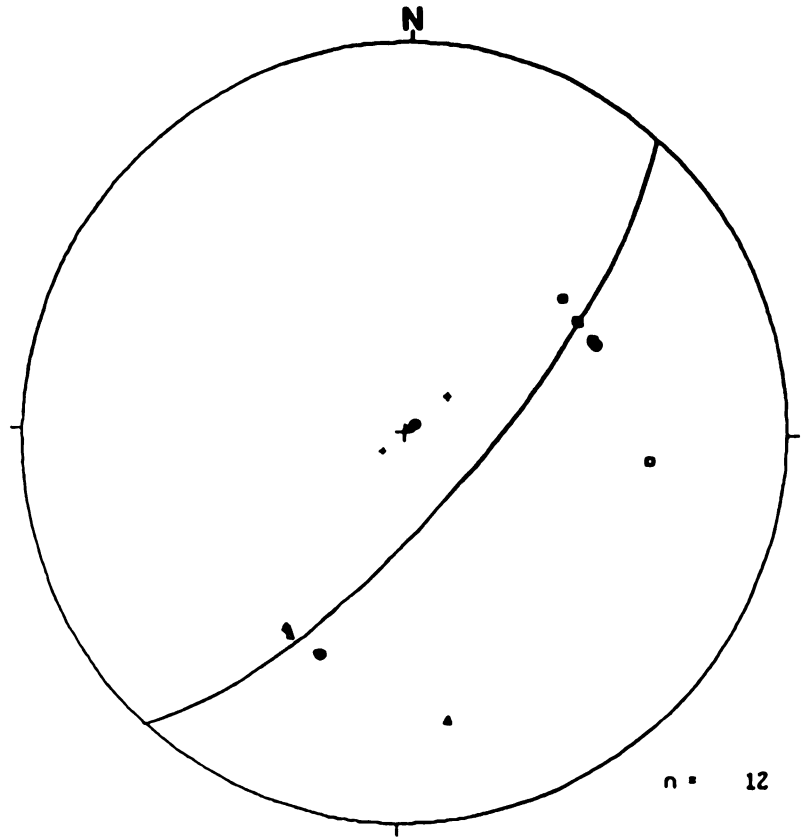

Figure 35. Stereo net plot of fractures from sample PL1. Squares represent fractures on PL1-1, triangles for PL1-2, and crosses for PL1-3. Solid circles are the mean orientations of the fracture traces for each plane. The plotted plane represents best fit plane of fracture.

TABLE 2: Mean fracture orientation on each of the three planes per sample.

Sample	Mean Fracture Orientation
MR1-1	045, 50
MR1-2	205, 57
MR1-3	208, 44
MR1 mean fracture: N36E, 82S	
MR2-1	020, 83
MR2-2	018, 41
MR2-3	186, 48
MR2 mean fracture: N13E, 86S	
MR3-1	014, 62
MR3-2	104, 84
MR3-3	003, 00
MR3 mean fracture: N3E, 84S	
MR9-1	285, 80
MR9-2	196, 87
MR9-3	007, 00
MR9 mean fracture: N7E, 85N	
MR10-1	280, 73
MR10-2	011, 81
MR10-3	213, 00
MR10 mean fracture: N32E, 80N	
PU1-1	206, 67
PU1-2	116, 67
PU1-3	009, 00
PU1 mean fracture: N8E, 82S	
BH1-1	150, 84
BH1-2	011, 00
BH1-3	060, 87
BH1 mean fracture: N11E, 87S	
PL1-1	065, 44
PL1-2	200, 39
PL1-3	050, 88
PL1 mean fracture: N40E, 74S	

Mean fracture orientation (calculated from the vector mean of all poles to fractures) is N18E, 87S.

Similar fractures on a larger scale are present along the north shore of the peninsula in the younger Copper Harbor conglomerate. These fractures are ubiquitous on the coastal exposure, range from appoximately five millimeters to tens of centimeters with the average approximatelv one centimeter, and most are filled with coarsely crystalline calcite while a small percentage are filled with quartz. Figures 36 through 38 show contoured stereo net plots of the poles to these fractures with the planes to the two most prominent contoured highs drawn in. The attitudes of these two planes are shown in Table 3.

Table 3

Outcrop fracture orientations along north shore of the Keweenawan Penninsula

Eagle River Area	N21E, 77S	N38W, 76S
Hebard Park Area	N14W, 66S	N78W, 65S
Copper Harbor Area	N8E, 80S	N57W, 77S

Approximately 95% of these fractures exhibit horizontal displacement only, the other 5% show a downward displacement of the north side relative to the south on the order of millimeters. The apparent vertical displacement is only common to the north-westerly striking fractures.

This fracture pattern in the upper conglomerate could represent two possibilities: first, since fractures in all three case are constrained to lie between the two prominent planes, they may represent extensional fractures which show more variation from the northerly trend of the fractures in thin section from the lower conglomerate, second, only the northerly trending fractures may be extensional-loading fractures, with the more north westerly fractures forming in response to unloading.

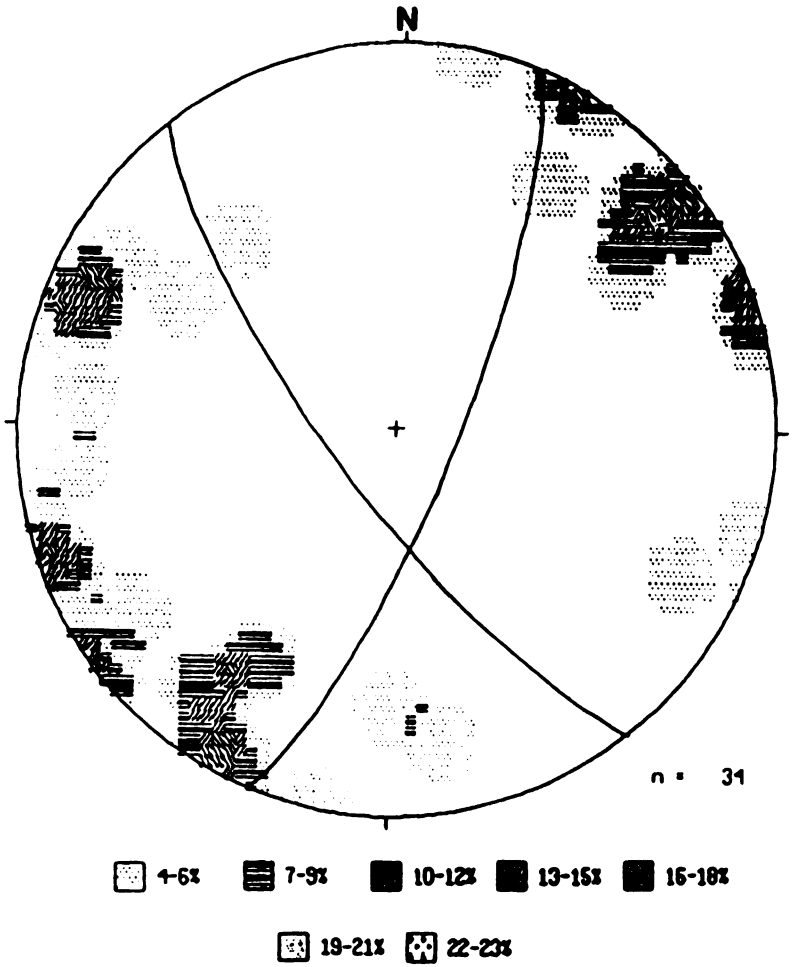

Figure 36. Contoured stereo net plot of fractures found along the Keweenaw peninsula north shore, near mouth of Eagle River.

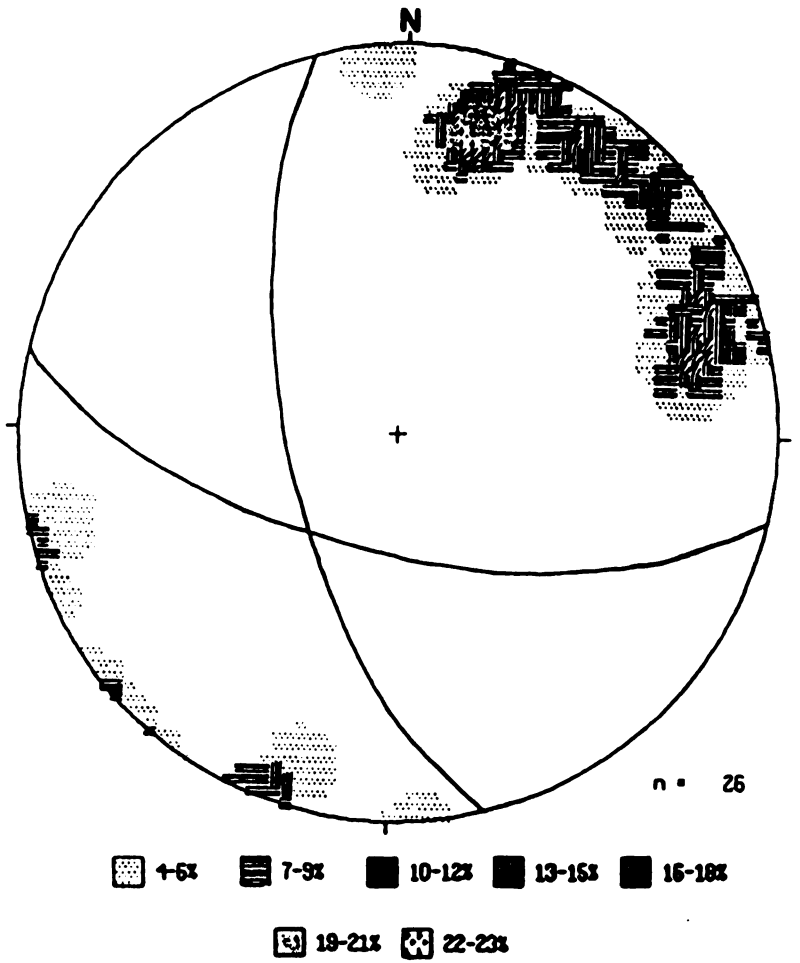

Figure 37. Contoured stereo net plot of fractures found along the Keweenaw peninsula north shore, near Hebard Park.

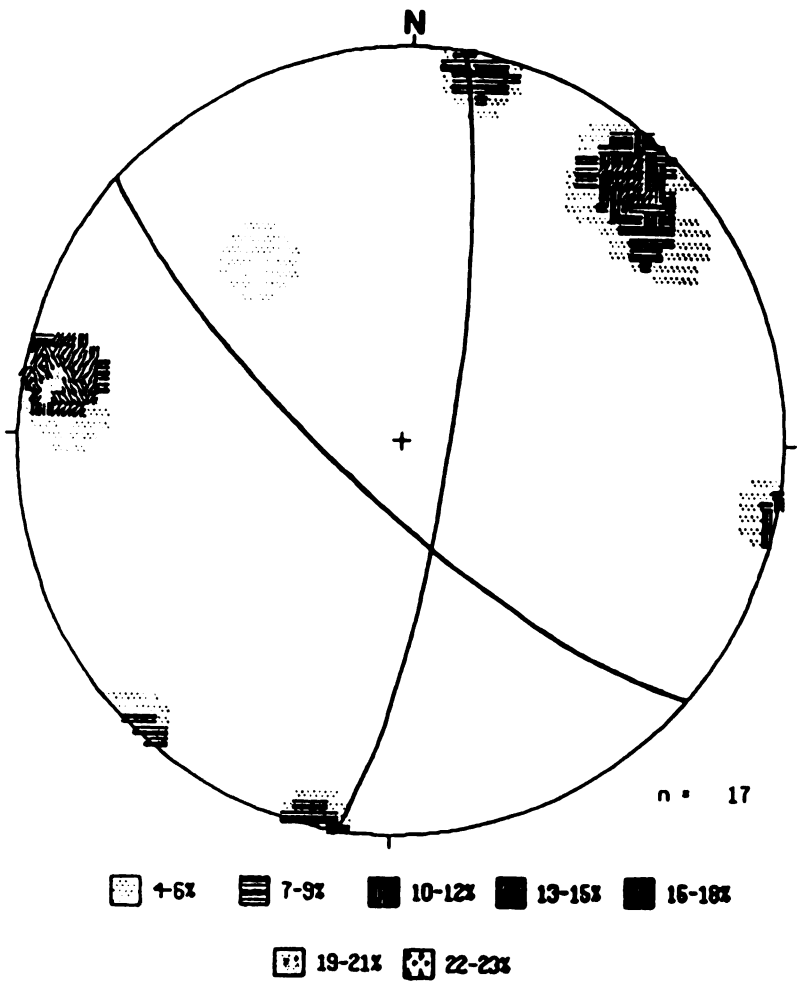

Figure 38. Contoured stereo net plot of fractures found along the Keweenaw peninsula north shore, near Copper Harbor.

Conclusions:

The Bohemia conglomerate and other unnamed conglomeratic beds in the deepest portion of the exposed Keweenawan sequence record a compressional phase of strain consistent with shortening in a north-south direction. Although the amount of strain is small, the orientation of the involved stresses suggests this compression resulted in the attitudes of both the steeply and gently dipping arms of the Lake Superior Syncline.

This direction of closure of the rifted portion of the continent does not support the impactogen model of rifting for the Midcontinent Rift system. This model requires the formation of large transform faults striking N45W in order to pull apart the crust into separate depositional basins. If these faults existed they would provide a zone of weakness for the compression to use, and we would expect to see shortening in that orientation instead of north-south.

A sheared origin is also precluded. This model would require a large shear zone striking in approximately the same direction as the transform faults in the impactogen model, supplying another structural weakness for later compression to reactivate.

The most likely model of origin for the Mid Continent Rift system is the a triple junction with a failed third arm. This allows separation of the crust in a north-south orientation, constrained by the arcuate arms of the system. Just as extension is constrained, so is the later closing phase, resulting in a syncline bound by compressional faults.

APPENDIX

APPENDIX A

STRAIN MEASUREMENTS FROM SAMPLES

The following table shows the data input to BESTELL. **Weight** is the mathematical weighting or preference applied to a given plane (1.00 in all cases of this study), **Major** refers to the length of the major axis of the strain ellipse for a given plane. **Minor** refers to the length of the minor axis of the strain ellipse for a given plane (normalized to 1.00 in this study), **Strike** is the azimuthal strike of the plane through the sample, **Dip** is the inclination in degrees from the horizontal - direction being determined using the right-hand rule of convention, **Input Pitch** and **Input AxRatio** refer, respectively, to the pitch of the vector mean Phi orientation in the plane and Major/Minor ratio as output from TRYELL. **Calculated Pitch** and **Calculated AxRatio** are BESTELL's recalculated Pitch and AxRatio from TRYELL's values in order to define three mutually perpendicular axes. **Undef Ellipse** is a measure of how closely the calculated strain ellipse value is to the measured strain value (1.00 being the ideal ratio of comparison) for each of the measured planes. **Log mean of undeformed ellipse** is a measure of how closely the calculated strain ellipse values combine to form a three dimensional ellipsoid (1.00 being a perfect ellipsoid).

TABLE 4: Measured (Input) and calculated (Output) strain axis orientations.

						INPUT		CALCULATED		Undef
BH1	Weight	Major	Minor	Strike	Dip	Pitch	AxRatio	Pitch	AxRatio	Ellipse
	1.00	1.83	1.00	330	90	131.1	1.83	132.8	1.83	1.04
	1.00	1.81	1.00	000	00	146.2	1.81	146.2	1.73	1.05
	1.00	1.82	1.00	060	90	078.4	1.82	079.2	1.89	1.05
	Log mean of undeformed ellipses = 1.044									

						INPUT		CALCULATED		Undef
BH1SL	Weight	Major	Minor	Strike	Dip	Pitch	AxRatio	Pitch	AxRatio	Ellipse
	1.00	1.72	1.00	330	90	124.8	1.72	130.7	1.69	1.12
	1.00	1.68	1.00	000	00	152.3	1.68	153.5	1.48	1.14
	1.00	1.84	1.00	060	90	115.2	1.84	111.8	1.98	1.12
	Log mean of undeformed ellipses = 1.126									

						INPUT		CALCULATED		Undef
PL1	Weight	Major	Minor	Strike	Dip	Pitch	AxRatio	Pitch	AxRatio	Ellipse
	1.00	1.83	1.00	320	45	125.4	1.83	123.2	1.86	1.05
	1.00	1.73	1.00	140	45	084.3	1.73	083.3	1.63	1.07
	1.00	1.67	1.00	050	90	167.9	1.67	165.3	1.71	1.06
	Log mean of undeformed ellipses = 1.059									

						INPUT		CALCULATED		Undef
MR10	Weight	Major	Minor	Strike	Dip	Pitch	AxRatio	Pitch	AxRatio	Ellipse
	1.00	1.73	1.00	280	90	063.3	1.73	043.7	1.68	1.45
	1.00	1.85	1.00	010	90	135.7	1.85	123.4	2.04	1.37
	1.00	1.80	1.00	000	00	106.6	1.80	127.2	1.62	1.50
	Log mean of undeformed ellipses = 1.441									

						INPUT		CALCULATED		Undef
MR10S1	Weight	Major	Minor	Strike	Dip	Pitch	AxRatio	Pitch	AxRatio	Ellipse
	1.00	1.78	1.00	280	90	055.6	1.78	047.4	1.76	1.19
	1.00	1.80	1.00	010	90	131.5	1.80	124.8	1.89	1.17
	1.00	1.81	1.00	000	00	127.5	1.81	135.9	1.73	1.20
	Log mean of undeformed ellipses = 1.186									

						INPUT		CALCULATED		Undef
MR9	Weight	Major	Minor	Strike	Dip	Pitch	AxRatio	Pitch	AxRatio	Ellipse
	1.00	1.68	1.00	285	90	008.0	1.68	006.8	1.85	1.11
	1.00	1.68	1.00	015	90	033.0	1.68	038.0	1.65	1.10
	1.00	1.80	1.00	000	00	104.9	1.80	104.8	1.62	1.11
	Log mean of undeformed ellipses = 1.105									

TABLE 4 (continued)

						INPUT		CALCULATED		Undef
MR3	Weight	Major	Minor	Strike	Dip	Pitch	AxRatio	Pitch	AxRatio	Ellipse
	1.00	1.70	1.00	014	90	038.0	1.70	041.1	1.69	1.06
	1.00	1.61	1.00	284	90	004.7	1.61	004.2	1.72	1.07
	1.00	1.75	1.00	000	00	096.6	1.75	095.4	1.64	1.07
	Log mean of undeformed ellipses - 1.067									

						INPUT		CALCULATED		Undef
MR2	Weight	Major	Minor	Strike	Dip	Pitch	AxRatio	Pitch	AxRatio	Ellipse
	1.00	1.89	1.00	020	90	030.2	1.89	031.6	2.07	1.11
	1.00	1.87	1.00	290	41	121.0	1.87	124.8	1.82	1.10
	1.00	1.98	1.00	110	49	166.2	1.96	163.5	1.83	1.11
	Log mean of undeformed ellipses - 1.103									

						INPUT		CALCULATED		Undef
MR2SL	Weight	Major	Minor	Strike	Dip	Pitch	AxRatio	Pitch	AxRatio	Ellipse
	1.00	1.98	1.00	020	90	021.3	1.98	012.8	1.79	1.25
	1.00	1.79	1.00	290	41	172.7	1.79	163.4	1.48	1.28
	1.00	1.90	1.00	110	49	158.7	1.90	163.2	2.23	1.22
	Log mean of undeformed ellipses - 1.250									

						INPUT		CALCULATED		Undef
MR1	Weight	Major	Minor	Strike	Dip	Pitch	AxRatio	Pitch	AxRatio	Ellipse
	1.00	1.77	1.00	295	54	163.0	1.77	149.6	1.57	1.31
	1.00	1.81	1.00	025	90	060.8	1.81	074.9	1.54	1.35
	1.00	1.91	1.00	115	46	150.3	1.91	156.5	2.18	1.24
	Log mean of undeformed ellipses - 1.301									

						INPUT		CALCULATED		Undef
PU1	Weight	Major	Minor	Strike	Dip	Pitch	AxRatio	Pitch	AxRatio	Ellipse
	1.00	1.92	1.00	296	90	083.0	1.92	052.4	1.60	1.84
	1.00	1.71	1.00	026	90	044.9	1.71	060.8	2.04	1.49
	1.00	1.63	1.00	000	00	099.7	1.63	085.4	1.63	1.28
	Log mean of undeformed ellipses - 1.523									

LIST OF REFERENCES

LIST OF REFERENCES

Anderson, S. L., and Burke, K., 1983. A Wilson cycle approach to some Proterozoic problems in eastern North America. Geological Society of America Memoir 161: 75-93

Bacon, L.O., 1966. Geologic structure east and south of the Keweenaw fault on the basis of geophysical evidence. In Steinhart, J. and Smith, T. eds., The earth beneath the continent: American Geophysical Union Geophysical Monograph 10, p. 42-55.

Behrendt, J., Green, A., Cannon, W., Hutchinson, D., Lee, M., Milkereit, B. Agena, W., Spencer, C., 1988. Crustal structure of the Midcontinent rift system: Results from GLIMPCE deep seismic reflection profiles. Geology, 16: 81-85.

Brown, L., Serpa, L., Setzer, T., Oliver, J., Kaufman, S., Lillie, R. Steiner, D., and Steeples, D. W., 1983. Intracrustal complexity in the United States midcontinent: Preliminary results from COCORP surveys in northeastern Kansas. Geology, 11: 25-30.

Burke, K. and Dewey, J. F., 1973. Plume-generated triple junctions: Key indicators in applying plate tectonics to old rocks. Journal of Geology, 81: 406-433.

Chase, C. G., and Gilmer, T. H., 1973. Precambrian plate tectonics: The midcontinent gravity high. Earth and Planetary Science Letters, v. 21, p. 71-78.

Daniels, P. A., Jr., 1982. Upper Precambrian sedimentary rocks: Oronto Group, Michigan Wisconsin. Geology and Tectonics of the Lake Superior Basin: GSA MEMOIR #156, 1982.

Dickas, A. B., 1986. Comparative Precambrian stratigraphy and structure along the Mid-Continent Rift. American Association of Petroleum Geologists Bulletin, v. 30, no.3: 225-238.

Dunnet, D. and Siddans, A.W.B., 1971. Non-random Sedimentary Fabrics and their modification by strain. Tectonphysics, 12: 307-325.

Freeman, B. and Lisle, R. J., 1987. The relationship between tectonic strain and the three dimensional shape of pebbles in deformed conglomerates. Journal of the Geological Society, London, 144: 635-639.

Gordon, M. B., and Hempton, M.R., 1986. Collision-induced rifting: The Grenville orogeny and the Keweenwan rift of North America. Tectonophysics, 127: 1-25.

LIST OF REFERENCES

Anderson, S. L., and Burke, K., 1983. A Wilson cycle approach to some Proterozoic problems in eastern North America. Geological Society of America Memoir 161: 75-93

Bacon, L.O., 1966. Geologic structure east and south of the Keweenaw fault on the basis of geophysical evidence. In Steinhart, J. and Smith, T. eds., The earth beneath the continent: American Geophysical Union Geophysical Monograph 10, p. 42-55.

Behrendt, J., Green, A., Cannon, W., Hutchinson, D., Lee, M., Milkereit, B. Agena, W., Spencer, C., 1988. Crustal structure of the Midcontinent rift system: Results from GLIMPCE deep seismic reflection profiles. Geology, 16: 81-85.

Brown, L., Serpa, L., Setzer, T., Oliver, J., Kaufman, S., Lillie, R. Steiner, D., and Steeples, D. W., 1983. Intracrustal complexity in the United States midcontinent: Preliminary results from COCORP surveys in northeastern Kansas. Geology, 11: 25-30.

Burke, K. and Dewey, J. F., 1973. Plume-generated triple junctions: Key indicators in applying plate tectonics to old rocks. Journal of Geology, 81: 406-433.

Chase, C. G., and Gilmer, T. H., 1973. Precambrian plate tectonics: The midcontinent gravity high. Earth and Planetary Science Letters, v. 21, p. 71-78.

Daniels, P. A., Jr., 1982. Upper Precambrian sedimentary rocks: Oronto Group, Michigan Wisconsin. Geology and Tectonics of the Lake Superior Basin: GSA MEMOIR #156, 1982.

Dickas, A. B., 1986. Comparative Precambrian stratigraphy and structure along the Mid-Continent Rift. American Association of Petroleum Geologists Bulletin, v. 30, no.3: 225-238.

Dunnet, D. and Siddans, A.W.B., 1971. Non-random Sedimentary Fabrics and their modification by strain. Tectonphysics, 12: 307-325.

Freeman, B. and Lisle, R. J., 1987. The relationship between tectonic strain and the three dimensional shape of pebbles in deformed conglomerates. Journal of the Geological Society, London, 144: 635-639.

Gordon, M. B., and Hempton, M.R., 1986. Collision-induced rifting: The Grenville orogeny and the Keweenwan rift of North America. Tectonophysics, 127: 1-25.

Halls, H. C., 1982. Crustal thickness in the Lake Superior region. Geology and Tectonics of the Lake Superior Basin: GSA MEMOIR *156, 1982.

Hinze, W J, Wold, R J, and O'Hara, N W, 1982. Gravity and magnetic anomaly studies of Lake Superior. Geology and Tectonics of the Lake Superior Basin. GSA MEMOIR *156, 1982.

Hobbs, B. E., Means, W. D., and Williams, P. F., An Outline of Structural Geology, 571 p., Wiley International, N.Y., 1976.

Jolly, W. T., and Smith, R E., 1971. Degradation and metamorphic differentiation of the Keweenawan tholeiitic lavas of Northern Michigan, U.S.A. Journal of Petrology, 13:273-309.

Kalliokosksi, J., 1982. Jacobsville Sandstone. Geology and Tectonics of the Lake Superior Basin. GSA MEMOIR *156, 1982.

Kalliokosksi, J., 1986. Calcium carbonate cement (caliche) in Keweenawan sedimentary rocks (~1 1 Ga), Upper Penninsula of Michigan. Precambrian Research, 32: 243-259.

Klasner, J. S., Cannon, W. F., and Van Schmus, W. R., 1982. The pre-Keweenawan tectonic history of southern Canadian Shield and its influence on formation of the Midcontinent Rift. Geology and Tectonics of the Lake Superior Basin: GSA MEMOIR *156, 1982.

Lisle, R. J., Geological strain analysis: a manual for the Rf/Phi method, Permagon Press, New York, N.Y. 1984.

McSwiggen, P.L., Morey, G. B., and Chandler, V. W., 1987. New model of the Midcontinent rift in eastern Minnesota and western Wisconsin. Tectonics, 6: 677-685.

Merk, G. P., and Jersa, M. A., 1982. Provenance and tectonic significance of the Keweenawan interflow sedimentary rocks. Geology and Tectonics of the Lake Superior Basin: GSA MEMOIR *156, 1982.

Morey, G. B., and Green, J. C., 1982. Status of the Keweenawan as a stratigraphic unit in the Lake Superior Region. Geology and Tectonics of the Lake Superior Basin: GSA MEMOIR *156, 1982.

Morey, G. B., and Ojakangas, R. W., 1982. Keweenawan sedimentary rocks of eastern Minnesota and northwestern Wisconsin. Geology and Tectonics of the Lake Superior Basin: GSA MEMOIR *156, 1982.

Mosher, S 1980. Pressure solution deformation of conglomerates in shear zones, Narrangansett Basin, Rhode Island. Journal of Structural Geology, 2: 218-225.

Ojakangas, R. W., and Morey, G. B., 1982. Keweenawan pre-volcanic quartz sandstones and related rocks of the Lake Superior region. Geology and Tectonics of the Lake Superior Basin: GSA MEMOIR *156, 1982.

Owens, W. H., 1984. The calculation of a best-fit ellipsoid from elliptical sections on arbitrarily oriented planes. Journal of Structural Geology, v. 6, no. 5: 571-578.

Palmason G. and Saemundsson, K., 1974. Iceland in relation to the Mid-Atlantic Ridge. Annual Review of Earth Planetary Sciences, 2: 22-50.

Ramsay, J. G., Folding and fracturing of rocks, McGraw-Hill. New York. N.Y. 1967.

Sanderson, D J., 1976. The superposition of compaction and plane strain Tectonophysics, 30: 35-54.

Sanderson, D J., and Marchini, W.R.D.1984. Transpression. Journal of Structural Geology, 6: 449-458.

Serpa, L., Setzer, T. Farmer, H., Brown, L., Oliver, J., Kaufman, S., Sharp, J, and Steeples, D. W. 1984. Structure of the southern Keweenawan rift from the COCORP surveys across the Midcontinent Geophysical Anomaly in northeastern Kansas. Tectonics, v. 3: 367-384.

Sims, P. K., Card, K. D., Morey, G. B., Peterman, Z. E., 1980. The Great Lakes tectonic zone a A major crustal structure in central North America. Geological Society of America Bulletin, 91: 690-698.

Van Shumas, W. R., and Hinze, W.J., 1985. The Midcontinent rift system: Annual Review of Earth Planetary Science, 13: 345-383.

Van Shumas, W. R., Green, J. C., and Halls, H. C., 1982. Geochronology of Keweenawan rocks in the Lake Superior Region, in Wold, R. J., and Hinz, W. J., eds. Geology and Tectonics of the Lake Superior Basin: GSA Memoir *156, 1982.

Watson, J., 1980. The origin and history of the Kapuskasing structural zone, Ontario, Canada. Canadian Journal of Earth Sciences, 17: 866-875.

Weiblen, P. W., 1982. Keweenawan intrusive igneous rocks. Geology and Tectonics of the Lake Superior Basin: GSA MEMOIR *156, 1982.

White, N., and McKenzie, D., 1988. Formation of the "steer's head" geometry of sedimentary basins by differential stretching of the crust and mantle. Geology, v.16: 250-253.

White, W. S., 1965. Tectonics of the Keweenawan basin, western Lake Superior region: U. S. Geological Survey Professional Paper 524-E, p. E1-E23.

White, W. S., 1966. Geological evidence for crustal structure in the western Lake Superior Basin. in Steinhart, J. S. and Smith, T. J., eds., The Earth Beneath the Continents: American Geophysical Union Geophysical Monograph 10, p. 1-28.

White, W. S., 1972. The base of the upper Keweenawan, Michigan and Wisconsin: U.S. Geological Survey Bulletin 1354-F, p. F1-F23.

Young, M. Y., 1980. The Grenville orogenic belt in the North Atlantic Continents. Earth-Science Reviews, 16: 277-288.